

# A Novel Self-Interference Cancellation Scheme for Channel-Unaware Differential Space-Time Two-Way Relay Networks

Salime Bameri, *Student Member, IEEE*, Siamak Talebi, Ramy H. Gohary<sup>ID</sup>, *Senior Member, IEEE*, and Halim Yanikomeroglu, *Fellow, IEEE*

**Abstract**—This paper considers channel-unaware two-way relay networks in which two single-antenna nodes exchange information via multiple non-regenerative relays, each with multiple antennas. A novel self-interference cancellation scheme for distributed differential space-time signalling is developed. Despite the absence of channel-state information, this scheme enables self-interference to be completely eliminated, thereby maximizing the signal-to-interference-plus-noise-ratio of the nodes. First, we obtain a lower bound on the pairwise error probability (PEP) under residual self-interference and we show that this bound approaches a non-zero constant at high signal-to-noise ratios (SNRs), indicating a zero diversity order and an asymptotic error floor. Second, we derive a necessary and sufficient condition for the proposed scheme to eliminate self-interference perfectly. Proper operation of this scheme requires the relays to have an even number of active antennas and for relays with odd number of active antennas, such a scheme does not exist. Third, we show that, when self-interference is cancelled perfectly, the error floor vanishes and an upper bound on the PEP approaches zero at high SNRs. In this case, it is shown that the diversity gain is equal to the number of relays and is independent of the number of antennas per relay. Finally, it is shown that the coding gain increases with increasing the number of antennas per relay and converges to a constant as the number of relay antennas becomes large.

**Index Terms**—Differential MIMO coding, two-way relay networks, half-duplex, amplify-and-forward, self-interference cancellation.

## I. INTRODUCTION

THE presence of multiple relays in wireless networks enables reliable communication of high data rates in many practical situations, notably those in which the channel between the source and destination is not line-of-sight with potentially deep fades [1]. One approach for the effective

utilization of multiple relays is to use distributed space-time (DST) codes [2], [3], whereby the relays organize their transmissions concurrently and autonomously so that the signals observed by the receiver possess a structure that facilitates reliable detection and efficient spectral utilization.

When the receiver has access to perfect channel-state information (CSI), the transmitter can use standard channel-aware signalling schemes [4], [5]. However, for the receiver to acquire such a CSI, the transmitter sends a prescribed set of training symbols, which are used by the receiver to estimate the channel. In some systems, transmitting training symbols and estimating the channel are not desirable. In those cases, it might be more attractive to use channel-unaware signalling schemes, i.e., schemes that do not require the receiver to have access to CSI.

A popular channel-unaware signalling scheme is the differential one. This scheme is suitable for signalling over continuously fading channels, which usually arise in mobile communications. In this scheme, the transmitter encodes information in the transition between the transmitted signal vectors, rather than in the vectors themselves [6]. Combining differential signalling with DST yields a differential DST (DDST) scheme that is suitable for channel-unaware relay networks [7].

Relay networks feature multiple relays, which operate either in a full-duplex mode, wherein each relay transmits and receives in the same frequency and time slots, or in a half-duplex mode, wherein transmission and reception occur either at different time slots or on different frequencies. Full-duplex relaying suffers from self-interference levels that are difficult to eliminate in practice. This renders half-duplex relaying more amenable to practical implementation. Relays operating in the half-duplex mode can be used to construct either one- or two-way relay networks [8], [9]. We will refer to the former as OWRNs and to the latter as TWRNs. In OWRNs, four phases are required for any two nodes to exchange their messages. Two phases are used for transmission from the first node to the second one and the remaining two phases are used for transmission in the reverse direction. Unfortunately, this transmission scheme renders OWRNs rather wasteful of the spectral resources available for communication. In contrast with OWRNs, in TWRNs, for two nodes to exchange information, they both send their messages to the relays simultaneously in the first phase. The relays process their received signals and in the second phase the relays broadcast

Manuscript received October 19, 2016; revised May 24, 2017 and September 14, 2017; accepted November 11, 2017. Date of publication December 6, 2017; date of current version February 9, 2018. This paper was presented at the 2017 IEEE International Workshop on Signal Processing Advances in Wireless Communications. The associate editor coordinating the review of this paper and approving it for publication was R. Brown. (Corresponding author: Ramy H. Gohary.)

S. Bameri and S. Talebi are with the Department of Electrical Engineering, Shahid Bahonar University of Kerman, Kerman 7616914111, Iran (e-mail: bameri@eng.uk.ac.ir; siamak.talebi@uk.ac.ir).

R. H. Gohary and H. Yanikomeroglu are with the Department of Systems and Computer Engineering, Carleton University, Ottawa, ON K1S 5B6, Canada (e-mail: ramy.gohary@gmail.com; halim@sce.carleton.ca).

Color versions of one or more of the figures in this paper are available online at <http://ieeexplore.ieee.org>.

Digital Object Identifier 10.1109/TWC.2017.2777446

a combination of these signals to both nodes [10]. Hence, it can be seen that TWRNs halves the number of phases required by ORNs to perform the same task. However, this advantage of TWRNs comes at the cost of additional processing at the nodes and/or the relays.

The fact that in TWRNs the two nodes send their signals to the relays on the same physical channel results in interference at the relays in the first communication phase, which upon broadcasting in the second phase, results in self-interference. Unless properly accounted for, self-interference can result in severe deterioration in the system performance, especially at high signal-to-noise ratios (SNRs). The effect of self-interference depends on the way in which the relays process their received signals. For ease of practical implementation, we will focus on the amplify-and-forward (AF) scheme, wherein the relays linearly process their received signals without attempting to regenerate the original messages. Other relaying schemes include the decode-and-forward (DF) and the compress-and-forward ones [1]. However, these schemes are significantly more computationally demanding and therefore less attractive than AF to implement in practice. To achieve desirable performance at high SNRs, it is necessary that the signalling scheme ensures that self-interfering signals are eliminated at the respective receivers. The difficulty of performing this task depends on CSI availability: when CSI is available, eliminating self-interference is straightforward, but when CSI is not available, eliminating self-interference constitutes a challenging problem, which will be addressed hereinafter.

Channel-unaware differential signalling in TWRNs has been considered in [11]–[13] for AF relays and in [13] and [14] for DF ones. The focus of the schemes in [11]–[13] was on TWRNs with one relay, which renders them not readily extensible nor amenable to space-time signalling and the diversity gains they provide. The case of TWRNs with multiple relays was considered in [14]. Therein a differential signalling scheme for DF relays with one antenna was devised. This scheme does not work for the multiple-antenna AF relays considered herein. In [15] a DDST signalling scheme [7] for systems with multiple single-antenna AF relays was developed. In this scheme, two-way communication is preceded by a one-way initialization procedure in which reference vectors are transmitted during the first four phases. In subsequent two-way communication, receivers perform differential detection depending on previous symbol decisions. This results in error propagation and deterioration in performance. Another class of signalling schemes for TWRNs with single-antenna AF relays was considered in [16]. In this class, DDST signalling is combined with blind channel estimation. The estimated channel is subsequently used by the nodes in the second communication phase to cancel the component of the received signal that arises from the signals they transmitted in the first phase. Because of blind estimation, the approach in [16] is prone to estimation errors and processing delays, cf. Section VII.

In this paper we consider a channel-unaware TWRN with two single-antenna nodes which communicate using differential signalling. In this TWRN, each AF half-duplex relay has multiple antennas [17]–[19]. For such TWRNs, we will

develop a novel self-interference cancellation scheme for DDST signalling in which each relay performs linear processing on its received signals jointly in space and time. This is in contrast with currently available processing strategies, which consider linear processing in time only. The novel scheme enables self-interference to be cancelled perfectly despite the fact that CSI is available neither at the nodes nor at the relays. In contrast, previously proposed self-interference cancellation schemes, e.g., the one proposed in [16], rely on channel estimation approaches. These approaches result in non-negligible residual interference, which subsequently inflicts serious degradation on the system performance. To show that, we derive a lower bound on the pairwise error probability (PEP) in the presence of residual self-interference and we show that this bound approaches a non-zero constant at high SNRs, i.e., the diversity gain is asymptotically equal to zero and an error floor occurs. Herein, we will show that such degradation can vanish by space-time processing of the relay received signals. In particular, it will be shown that a special design for the space processing matrix will cancel self-interference perfectly and will subsequently maximize the signal-to-interference-plus-noise-ratio (SINR) observed by the nodes. Our analysis shows that perfect cancellation is not possible if any relay were to have an odd number of active antennas. To capture the effect of perfect cancellation on the system performance, we derive an upper bound on the PEP. This bound shows that, first, at high SNRs, the proposed scheme achieves a diversity gain equal to the number of relays, but is independent of the number of relay antennas. Second, this scheme achieves a coding gain that increases with the number of relay antennas. Finally, we show that the system performance converges with the number of relay antennas, suggesting that increasing the number of relays is more beneficial than increasing the number of antennas per relay. In summary:

- we propose a novel relaying scheme for DDST signalling in which the relays process their received signals in space and time, rather than in time only, as in currently available work;
- we derive a lower bound on the PEP to show that any non-zero residual self-interference results in an error floor and zero diversity order;
- we design a signalling methodology that enables the relays to cancel self-interference perfectly without invoking CSI estimation, provided that each relay has an even number of active antennas (such a scheme is not feasible if the number of antennas is odd); and
- we derive an upper bound on the PEP yielded by the proposed scheme and we show that the diversity gain is equal to the number of relays, and is independent of the (even) number of relay antennas. In contrast, the coding gain increases with the number of antennas per relay and converges to a constant when the number of relay antennas goes to infinity.

The paper is organized as follows. Section II, presents the system model and the DDST signalling scheme. In Section III, we propose a novel space-time relaying scheme. The effect of self-interference on the system performance is analyzed

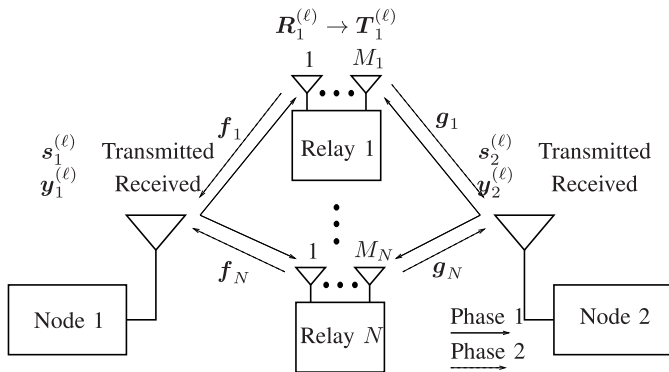


Fig. 1. Block diagram of a TWRN.

in Section IV. Conditions for ensuring perfect self-interference cancellation are derived in Section V. Section VI analyses the system performance when self-interference is cancelled perfectly. Section VII provides simulation results. Section VIII summarizes the key differences between our scheme and the one in [16] and Section IX concludes the paper. For convenience, proofs are relegated to the appendix.

*Notations:* we use bold upper and lower case letters to denote matrices and column vectors, respectively. The real and imaginary parts are denoted by  $\Re(\cdot)$  and  $\Im(\cdot)$ , respectively. The conjugate, transpose, Hermitian, trace and determinant of a matrix  $\mathbf{A}$  are denoted by  $\overline{\mathbf{A}}$ ,  $\mathbf{A}^T$ ,  $\mathbf{A}^\dagger$ ,  $\text{Tr}(\mathbf{A})$  and  $|\mathbf{A}|$ , respectively. The direct sum of matrices  $\mathbf{A}_i$  is denoted by  $\bigoplus_i \mathbf{A}_i$ .

## II. SYSTEM MODEL

We consider a channel-unaware half-duplex TWRN with two single-antenna nodes and  $N$  AF relays as shown in Figure 1. The  $n$ -th relay has  $M_n$  antennas which are used for both transmission and reception,  $n = 1, \dots, N$ . The vector channel between node 1 and the  $n$ -th relay is denoted by  $\mathbf{f}_n \in \mathbb{C}^{M_n}$  and the corresponding channel for node 2 is denoted by  $\mathbf{g}_n \in \mathbb{C}^{M_n}$ . The  $m$ -th entry of  $\mathbf{f}_n$  and the corresponding entry of  $\mathbf{g}_n$  represent the channel between node 1 and node 2, and the  $m$ -th antenna of relay  $n$ , respectively,  $m = 1, \dots, M_n$ ,  $n = 1, \dots, N$ . The channels are assumed to be block Rayleigh fading and hence the entries of the channel vectors  $\{\mathbf{f}_n\}$  and  $\{\mathbf{g}_n\}$  are Gaussian distributed with zero mean and unit variance, i.e.,  $\mathbb{E}\{\mathbf{f}_n \mathbf{f}_n^\dagger\} = \mathbb{E}\{\mathbf{g}_n \mathbf{g}_n^\dagger\} = \mathbf{I}_{M_n}$ .

In the considered channel-unaware TWRN, neither the nodes nor the relays have access to CSI prior to detection. In this scenario, a convenient means for communication is the one offered by DDST. This scheme was used in [16] in channel-unaware signalling for the case when the relays have one antenna each. Unfortunately, the scheme proposed in [16] does not eliminate self-interference completely, resulting in a zero diversity gain, as will be shown below. To overcome this drawback, we herein use DDST, but with multiple antennas at each relay. For this scenario we will develop a signalling scheme that achieves a high-SNR diversity gain equal to the number of relays. The new relaying scheme is based on a novel approach for eliminating self-interference perfectly at the multiple-antenna AF relays. Each relay linearly processes its

received signal matrix containing the components transmitted from both nodes in the first phase and generates a new matrix, which is subsequently broadcast to the nodes in the second phase. The linear combinations at the relays are organized in such a way that the signal received at each of the two destination nodes appears as if it were generated by a particular space-time code.

We will consider two classes of DST codes involving linear and sesquilinear<sup>1</sup> combinations of the transmitted symbols. Instances of the first class include real orthogonal codes [4], whereas instances of the second class include the Alamouti and the  $SP(2)$  codes [7]. Detection for both classes is similar but transmission is slightly different as we elaborate below.

In both the linear and sesquilinear classes, the nodes organize their transmissions in  $L$  blocks of  $N$  symbols, each denoted by the  $N \times 1$  vector,  $\mathbf{s}_i^{(\ell)}$ ,  $i = 1, 2$ ,  $\ell = 1, \dots, L - 1$ . More precisely, similar to [7], in the  $\ell$ -th block, each node differentially encodes its message as follows

$$\mathbf{s}_i^{(\ell)} = \mathbf{U}_i^{(\ell)} \mathbf{s}_i^{(\ell-1)}, \quad i = 1, 2, \quad \ell = 1, \dots, L - 1, \quad (1)$$

where  $\mathbf{U}_i^{(\ell)}$  is a unitary  $N \times N$  matrix to which the message of node  $i$  in the  $\ell$ -th block is mapped, and  $\mathbf{s}_i^{(0)}$  is an arbitrary initialization vector, which is not required to be known *a priori*. The vectors  $\{\mathbf{s}_i^{(\ell)}\}$  are normalized so that  $\mathbb{E}\{\mathbf{s}_i^{(\ell)} \mathbf{s}_i^{(\ell)\dagger}\} = \mathbf{I}_N$ ,  $i = 1, 2$ ,  $\ell = 1, \dots, L - 1$ .

### A. First Transmission Phase

In the first TWRN transmission phase, the nodes transmit their messages to the two-way relays. The particular structure of the signals emitted by the nodes depends on the class of signalling, linear or sesquilinear. We will discuss these classes separately.

1) *The Class of Linearly-Structured Codes:* In this class, node  $i$  transmits the  $\ell$ -th block  $\mathbf{s}_i^{(\ell)}$ ,  $i = 1, 2$ , during  $N$  symbol durations. Hence, the received signal of the  $n$ -th relay, is given by

$$\mathbf{R}_n^{(\ell)} = \sqrt{P_1} \mathbf{s}_1^{(\ell)} \mathbf{f}_n^T + \sqrt{P_2} \mathbf{s}_2^{(\ell)} \mathbf{g}_n^T + \mathbf{V}_n^{(\ell)}, \quad n = 1, \dots, N, \quad \ell = 1, \dots, L - 1, \quad (2)$$

where the  $m$ -th column of  $\mathbf{R}_n^{(\ell)} \in \mathbb{C}^{N \times M_n}$ , denoted by  $\mathbf{r}_{nm}^{(\ell)}$ , is the  $N \times 1$  received vector at the  $m$ -th antenna of the  $n$ -th relay,  $P_i$  is the average power of node  $i$ ,  $i = 1, 2$ , and  $\mathbf{V}_n^{(\ell)} \in \mathbb{C}^{N \times M_n}$  is the noise matrix observed during the  $\ell$ -th block at the  $n$ -th relay. Throughout, the entries of  $\mathbf{V}_n^{(\ell)}$  are assumed to be Gaussian with zero mean and unit variance, whence  $\mathbb{E}\{\text{Tr}(\mathbf{V}_n^{(\ell)\dagger} \mathbf{V}_n^{(\ell)})\} = NM_n$ .

2) *The Class of Sesquilinearly-Structured Codes:* In this class, node  $i$  transmits the  $\ell$ -th block  $\mathbf{s}_i^{(\ell)}$  followed by its complex conjugate,  $\overline{\mathbf{s}}_i^{(\ell)}$ ,  $i = 1, 2$ . As we elaborate below, this step is necessary because otherwise, the relay, being non-regenerative, would not be able to eliminate self-interference perfectly without CSI. In this case, nodes consume  $2N$  symbol durations for transmitting the same information and the

<sup>1</sup>Sesquilinear combinations refer to those combinations that are linear in the symbols and their complex conjugates.

received signal of the  $n$ -th relay,  $\mathbf{R}_n^{(\ell)}$ , is given by

$$\mathbf{R}_n^{(\ell)} = \sqrt{P_1}[\mathbf{s}_1^{(\ell)T}, \bar{\mathbf{s}}_1^{(\ell)T}]^T \mathbf{f}_n^T + \sqrt{P_2}[\mathbf{s}_2^{(\ell)T}, \bar{\mathbf{s}}_2^{(\ell)T}]^T \mathbf{g}_n^T + \mathbf{V}_n^{(\ell)}, \quad n = 1, \dots, N, \quad \ell = 1, \dots, L-1, \quad (3)$$

where the definitions of  $\mathbf{R}_n^{(\ell)}$ ,  $\{P_i\}$  and  $\mathbf{V}_n^{(\ell)}$  are the same as in the previous case, with the exception that  $\mathbf{R}_n^{(\ell)} \in \mathbb{C}^{2N \times M_n}$  and  $\mathbf{V}_n^{(\ell)} \in \mathbb{C}^{2N \times M_n}$ , whence  $\mathbb{E}\{\text{Tr}(\mathbf{V}_n^{(\ell)\dagger} \mathbf{V}_n^{(\ell)})\} = 2NM_n$ .

### B. Linear Processing at the Relays and the Second Transmission Phase

The relays, being non-regenerative, process their received signals without attempting to recover the signals transmitted from the nodes in the first phase. We will consider the case in which the relays perform linear processing on these signals. This approach was considered in [2], [7], [10], [16], [20], and [21], but processing in these references is performed in the time domain. Unlike the aforementioned references, herein we consider a general approach in which processing is performed jointly over space and time, as will be elaborated below.

Let the linear transformation at the  $n$ -th relay be denoted by  $\mathbb{T}_n : \mathbf{R}_n^{(\ell)} \mapsto \mathbf{T}_n^{(\ell)}$ , i.e.,  $\mathbb{T}_n$  maps the received matrix of the  $n$ -th relay during the  $\ell$ -th block to the matrix  $\mathbf{T}_n^{(\ell)} \in \mathbb{C}^{N \times M_n}$ . Our objective is to identify and analyze appropriate choices for  $\mathbb{T}_n$  for both classes of codes.

Upon receiving the entire matrix  $\mathbf{R}_n^{(\ell)}$  at the end of the  $\ell$ -th block, the  $n$ -th relay generates and broadcasts  $\mathbf{T}_n^{(\ell)}$  to the two nodes. The received signals of these nodes can be expressed as:

$$\mathbf{y}_1^{(\ell)} = \sum_{n=1}^N \mathbf{T}_n^{(\ell)} \mathbf{f}_n + \mathbf{z}_1^{(\ell)}, \quad \mathbf{y}_2^{(\ell)} = \sum_{n=1}^N \mathbf{T}_n^{(\ell)} \mathbf{g}_n + \mathbf{z}_2^{(\ell)}, \quad (4)$$

where  $\mathbf{z}_i^{(\ell)}$  are the  $N \times 1$  noise vectors at the  $i$ -th node during the  $\ell$ -th received block.

The precise definition of  $\{\mathbf{T}_n^{(\ell)}\}$  will be given in the next section. For now, however, we note that, because of linear processing at the relays, each of the matrices  $\{\mathbf{T}_n^{(\ell)}\}$  contains two components (cf. Figure 1): the first corresponds to the desired signal of node  $i$  which is transmitted by the other node, and the second corresponds to the self-interference generated by node  $i$ 's own transmission in the first phase,  $i = 1, 2$ . In the next section, we will show that self-interference heavily impacts the system performance and unless perfectly cancelled, it will cause the high-SNR diversity gain to be zero. To alleviate this drawback, we will develop a signalling strategy that ensures achieving a diversity gain equal to the number of relays.

## III. JOINT RELAY PROCESSING IN SPACE AND TIME

In the original DDST signalling, processing at the  $n$ -th relay,  $\mathbb{T}_n$ , is performed in the time domain only even when the relays have multiple antennas [2]. We will show that this signalling strategy will prevent self-interference from being perfectly cancelled. In particular, we will show that, if the number of active antennas at any relay is odd, temporal processing alone does not suffice to cancel self-interference perfectly.

To alleviate this drawback, in this section, we develop a novel signalling approach for performing linear processing at the relays jointly in space and time. In particular, we define  $\mathbb{T}_n$  to be the linear transformation that maps  $\mathbf{R}_n^{(\ell)}$  to  $\mathbf{T}_n^{(\ell)}$  via

$$\mathbf{T}_n^{(\ell)} = \beta_n \mathbf{C}_n \mathbf{R}_n^{(\ell)} \mathbf{X}_n, \quad \mathbf{X}_n \in \mathbb{C}^{M_n \times M_n}, \quad n = 1, \dots, N. \quad (5)$$

To ensure that the average transmission power of relay  $n$  is equal to a given power budget,  $P_{r_n}$ , the scalars  $\{\beta_n\}$  must satisfy  $\beta_n = \sqrt{\frac{NP_{r_n}}{\mathbb{E}\{\text{Tr}(\mathbf{C}_n \mathbf{R}_n^{(\ell)} \mathbf{X}_n \mathbf{X}_n^\dagger \mathbf{R}_n^{(\ell)\dagger} \mathbf{C}_n^\dagger)\}}}$ . The matrices  $\{\mathbf{X}_n\}$

in (5) are used for processing in the space domain and the matrices  $\{\mathbf{C}_n\}$  are used for processing in the time domain. To ensure that the relay power constraints are satisfied, we have

$$\text{Tr}(\mathbf{C}_n \mathbf{C}_n^\dagger) = N. \quad (6)$$

The structure of  $\{\mathbf{C}_n\}$  is different for linear and sesquilinear codes. In particular,

$$\mathbf{C}_n = \begin{cases} \mathbf{A}_n, & \text{for linear codes, } n = 1, \dots, N, \\ \begin{bmatrix} \mathbf{A}_n & \\ & \mathbf{B}_n \end{bmatrix}, & \text{for sesquilinear codes, } n = 1, \dots, N. \end{cases} \quad (7)$$

The choice of  $\mathbf{A}_n, \mathbf{B}_n \in \mathbb{C}^{N \times N}$  depends on the space-time code used in the network, see e.g., [7]. For example, for the  $2 \times 2$  linear real-orthogonal DST code,  $\mathbf{A}_1 = \mathbf{I}_2$  and  $\mathbf{A}_2 = \mathbf{J}$ , where

$$\mathbf{J} = \begin{bmatrix} 0 & -1 \\ 1 & 0 \end{bmatrix}, \quad (8)$$

and, for the  $2 \times 2$  sesquilinear Alamouti DST code,  $\mathbf{A}_1 = \mathbf{I}_2$ ,  $\mathbf{B}_1 = \mathbf{0}$ ,  $\mathbf{A}_2 = \mathbf{0}$  and  $\mathbf{B}_2 = \mathbf{J}$ .

The matrices  $\{\mathbf{A}_n\}_{n=1}^N$ ,  $\{\mathbf{B}_n\}_{n=1}^N$  and  $\{\mathbf{X}_n\}_{n=1}^N$  must satisfy the power constraints. In addition, since the channels  $\{\mathbf{f}_n\}$  and  $\{\mathbf{g}_n\}$  in (2)–(4) are isotropically distributed (i.d.) and CSI is not available, maintaining the channels to be i.d. requires these matrices to be unitary. Otherwise, the power distribution across the relay antennas will be nonuniform, which compromises performance if high power is allocated to weak channels [2], [7], [21]–[23].

In addition to unitarity,  $\{\mathbf{A}_n\}$ ,  $\{\mathbf{B}_n\}$  and  $\{\mathbf{X}_n\}$  must satisfy other constraints. In particular, for the receivers to use the signal received in the  $(\ell - 1)$ -th block to detect the signal received in the  $\ell$ -th block, the matrices  $\{\mathbf{A}_n\}$  and  $\{\mathbf{B}_n\}$ , must commute with  $\{\mathbf{U}_i^{(\ell)}\}$  in (1) [7], i.e.,

$$\mathbf{U}_i^{(\ell)} \mathbf{A}_n = \mathbf{A}_n \mathbf{U}_i^{(\ell)}, \quad \text{and} \quad \mathbf{U}_i^{(\ell)} \mathbf{B}_n = \mathbf{B}_n \bar{\mathbf{U}}_i^{(\ell)}, \quad i = 1, 2, \quad n = 1, \dots, N, \quad \ell = 1, \dots, L-1. \quad (9)$$

These relationships will be assumed to hold throughout. As for  $\{\mathbf{X}_n\}$ , in Section V, we will derive additional conditions to ensure that these matrices can effect perfect elimination of self-interference despite the absence of CSI at the receivers.

To proceed with analysis, we use (4), (5) and (9) to express the  $N \times 1$  received signal of node 1 in the following form; analysis for node 2 follows from symmetry.

$$\mathbf{y}_1^{(\ell)} = \sqrt{P_1} \mathbf{S}_1^{(\ell)} \mathbf{h}_1 + \sqrt{P_2} \mathbf{S}_2^{(\ell)} \mathbf{h}_2 + \mathbf{w}_1^{(\ell)}, \quad (10)$$

where the  $N \times N$  matrices  $\{\mathbf{S}_i^{(\ell)}\}$  are given by

$$\mathbf{S}_i^{(\ell)} = [\mathbf{C}_1 \boldsymbol{\theta}_i^{(\ell)}, \dots, \mathbf{C}_N \boldsymbol{\theta}_i^{(\ell)}] \in \mathbb{C}^{N \times N},$$

$$i = 1, 2, \quad \ell = 1, \dots, L-1, \quad (11)$$

$$\boldsymbol{\theta}_i^{(\ell)} = \begin{cases} \mathbf{s}_i^{(\ell)}, & \text{for linear codes, } i = 1, 2, \\ \begin{bmatrix} \mathbf{s}_i^{(\ell)T} & \bar{\mathbf{s}}_i^{(\ell)T} \end{bmatrix}^T & \text{for sesquilinear codes, } i = 1, 2, \end{cases} \quad (12)$$

the  $N \times 1$  equivalent channel and noise vectors,  $\mathbf{h}_1$ ,  $\mathbf{h}_2$  and  $\mathbf{w}_1^{(\ell)}$  are respectively given by

$$\mathbf{h}_1 = [\beta_1 \mathbf{f}_1^T \mathbf{X}_1 \mathbf{f}_1, \dots, \beta_N \mathbf{f}_N^T \mathbf{X}_N \mathbf{f}_N]^T,$$

$$\mathbf{h}_2 = [\beta_1 \mathbf{g}_1^T \mathbf{X}_1 \mathbf{f}_1, \dots, \beta_N \mathbf{g}_N^T \mathbf{X}_N \mathbf{f}_N]^T, \quad (13)$$

$$\mathbf{w}_1^{(\ell)} = \sum_{n=1}^N \beta_n \mathbf{C}_n \mathbf{V}_n^{(\ell)} \mathbf{X}_n \mathbf{f}_n + \mathbf{z}_1^{(\ell)}. \quad (14)$$

The first term on the right hand side (RHS) of (10) characterizes the signal transmitted by the same node during the first phase, that is, this term comprises self-interference. The second term characterizes the signal transmitted by the other node (i.e., node 2) during the first phase, and hence, this term comprises the desired signal. Finally, the third term characterizes the equivalent noise, which, from (14), contains contributions from the first and second transmission phases. Using statistical independence of  $\{\mathbf{f}_n\}$  and  $\{\mathbf{V}_n^{(\ell)}\}$ , we have  $\mathbf{E}\{\mathbf{w}_1^{(\ell)}\} = \mathbf{0}$  and, cf. Appendix A-A,

$$\boldsymbol{\Sigma}_{\mathbf{w}_1} = \mathbf{E}\{\mathbf{w}_1^{(\ell)} \mathbf{w}_1^{(\ell)\dagger}\} = \sum_{n=1}^N \beta_n^2 M_n \mathbf{C}_n \mathbf{C}_n^\dagger + \mathbf{I}_N. \quad (15)$$

Since  $\{\mathbf{f}_n\}$  are random and unknown and  $\{\mathbf{V}_n^{(\ell)}\}$  are Gaussian distributed, the distribution of the equivalent noise  $\mathbf{w}_1^{(\ell)}$  depends on the distribution of  $\{\mathbf{f}_n\}$  and is generally not Gaussian. Finding the exact distribution of  $\mathbf{w}_1^{(\ell)}$  is not only difficult, but might also prohibit drawing insight into the key elements that govern performance. To alleviate this difficulty, we will follow the approach in [7] to approximate  $\mathbf{w}_1^{(\ell)}$  by a Gaussian random vector with zero mean and the covariance in (15). In fact, using the central limit theorem it can be verified that the distribution of  $\mathbf{w}_1^{(\ell)}$  approaches the Gaussian one as  $M_n$  grows,  $\forall n$ . This approximation will be used throughout.

#### IV. SYSTEM PERFORMANCE ANALYSIS IN THE PRESENCE OF SELF-INTERFERENCE

In this section, we show that self-interference causes both the SINR and the PEP to converge to finite strictly positive constants as the signalling power increases. This implies that, without perfect cancellation of self-interference, the diversity gain is asymptotically zero. Suppose that the received signal in (10) includes a fraction,  $\zeta \in (0, 1]$ , of the self-interference component, i.e.,

$$\mathbf{y}_1^{(\ell)} = \zeta \sqrt{P_1} \mathbf{S}_1^{(\ell)} \mathbf{h}_1 + \sqrt{P_2} \mathbf{S}_2^{(\ell)} \mathbf{h}_2 + \mathbf{w}_1^{(\ell)}. \quad (16)$$

For ease of exposition, we assume that the power of both nodes and each relay is a scalar multiple of a constant power,  $P$ , i.e.,  $P_1 = P$ ,  $P_2 = \delta_0 P$ ,  $P_{r_n} = \delta_n P$ , where  $\delta_n > 0$ ,  $\forall n$ . Using the

unitarity of  $\mathbf{X}_n$  along with the expressions in (2), (3) and (6) yields

$$\beta_n = \sqrt{\frac{\delta_n P}{M_n((1 + \delta_0)P + 1)}}. \quad (17)$$

##### A. The Effect of Self-Interference on SINR

To illustrate the effect of self-interference on the novel signalling scheme, we compute the average SINR of node 1. Analogous computation for node 2 is *mutatis mutandis*. Using (11)–(13), in Appendix A-B we show that the average power of the desired signal in (16) is

$$\mathbf{E}\{(\mathbf{S}_2^{(\ell)} \mathbf{h}_2)^\dagger (\mathbf{S}_2^{(\ell)} \mathbf{h}_2)\} = N \sum_{n=1}^N \beta_n^2 M_n. \quad (18)$$

For the average power of self-interference in (16), in Appendix A-C we show that

$$\mathbf{E}\{(\mathbf{S}_1^{(\ell)} \mathbf{h}_1)^\dagger (\mathbf{S}_1^{(\ell)} \mathbf{h}_1)\} = N \sum_{n=1}^N \beta_n^2 \alpha_n, \quad (19)$$

$$\alpha_n = 2 \sum_{k=1}^{M_n} |x_{kk}^{(n)}|^2 + \sum_{k=1}^{M_n} \sum_{j=k+1}^{M_n} |x_{kj}^{(n)} + x_{jk}^{(n)}|^2, \quad n = 1, \dots, N, \quad (20)$$

and  $x_{lk}^{(n)}$  is the  $lk$ -th entry of  $\mathbf{X}_n$ . Finally, using (15) and (6), we have

$$\mathbf{E}\{\mathbf{w}_1^{(\ell)\dagger} \mathbf{w}_1^{(\ell)}\} = \text{Tr}(\mathbf{E}\{\mathbf{w}_1^{(\ell)} \mathbf{w}_1^{(\ell)\dagger}\}) = N \sum_{n=1}^N \beta_n^2 M_n + N. \quad (21)$$

From (18), (19) and (21), the average SINR observed by node 1 can be readily seen to be

$$\text{SINR} = \frac{\delta_0 P^2 \sum_{n=1}^N \delta_n}{\zeta^2 P^2 \sum_{n=1}^N \frac{\alpha_n \delta_n}{M_n} + (1 + \sum_{n=0}^N \delta_n) P + 1}. \quad (22)$$

Using (22), it can be seen that  $\lim_{P \rightarrow \infty} \text{SINR} = \frac{\delta_0 \sum_{n=1}^N \delta_n}{\zeta^2 \sum_{n=1}^N \frac{\alpha_n \delta_n}{M_n}}$ .

Thus, if self-interference is not perfectly cancelled at any of the relays, the SINR will converge to a strictly positive constant.

##### B. Lower Bound on PEP

To investigate the effect of self-interference on the error rate of the scheme proposed in Section III, we will derive a lower bound on the PEP. We will show that, under general conditions, this bound converges to a strictly positive constant that does not depend on  $P$ , unless self-interference is perfectly cancelled. In other words, any self-interference causes an error floor. Our main result of this section is recorded in Theorem 1.

*Theorem 1:* Let  $\mathbf{h}_1$ ,  $\mathbf{h}_2$  and  $\mathbf{w}_1$  in (10) be zero mean Gaussian random vectors with average covariance matrices that are given by  $\boldsymbol{\Sigma}_{\mathbf{h}_1} = \text{diag}(\beta_1^2 \alpha_1, \dots, \beta_N^2 \alpha_N)$ ,  $\boldsymbol{\Sigma}_{\mathbf{h}_2} = \text{diag}(\beta_1^2 M_1, \dots, \beta_N^2 M_N)$  and (15), respectively. Consider the two distributed space-time codewords  $\mathbf{S}_{2,a}^{(\ell)}$  and  $\mathbf{S}_{2,b}^{(\ell)}$ . Let  $\sigma_{\max}^{(a,b)}$

be the largest eigenvalue of  $(\mathbf{S}_{2,a}^{(\ell)} - \mathbf{S}_{2,b}^{(\ell)})^\dagger (\mathbf{S}_{2,a}^{(\ell)} - \mathbf{S}_{2,b}^{(\ell)})$  and let  $\hat{\sigma}_{\max} = \max_{a,b} \sigma_{\max}^{(a,b)}$ . In addition, let  $\lambda_{\min}(\boldsymbol{\theta}_1)$  and  $\mu_{\min}^{(n)}$  be the smallest eigenvalues of  $\sum_{n=1}^N \frac{\alpha_n \delta_n}{M_n} \mathbf{C}_n \boldsymbol{\theta}_1^{(\ell)} \boldsymbol{\theta}_1^{(\ell)\dagger} \mathbf{C}_n^\dagger$  and  $\mathbf{C}_n \mathbf{C}_n^\dagger$ , respectively. Then, the probability of mistaking  $\mathbf{S}_{2,a}^{(\ell)}$  for  $\mathbf{S}_{2,b}^{(\ell)}$  satisfies:

$$\Pr(\mathbf{S}_{2,a}^{(\ell)} \rightarrow \mathbf{S}_{2,b}^{(\ell)}) \geq \mathbb{E}_{\boldsymbol{\theta}_1^{(\ell)}} \{ \mathcal{Q}(\sqrt{\Delta_1}) \},$$

$$\Delta_1 \triangleq \frac{2^{-1} \delta_0 \hat{\sigma}_{\max} \sum_{n=1}^N \delta_n}{\zeta^2 \lambda_{\min}(\boldsymbol{\theta}_1^{(\ell)}) + (1 + \delta_0 + \sum_{n=1}^N \delta_n \mu_{\min}^{(n)}) P^{-1} + P^{-2}}. \quad (23)$$

*Proof:* See Appendix B. ■

First, we note that  $\lambda_{\min}(\boldsymbol{\theta}_1^{(\ell)})$  and  $\mu_{\min}^{(n)}$  do not depend on  $P$ . Furthermore, we note that, for both the linear and sesquilinear cases,  $\mathbf{C}_n \boldsymbol{\theta}_1^{(\ell)}$  is an  $N$ -dimensional vector,  $n = 1, \dots, N$ , cf. (7), (12). Hence, if for the proposed relaying scheme and for some  $\boldsymbol{\theta}_1^{(\ell)}$ , the matrices  $\{\mathbf{C}_n\}_{n=1}^N$  are such that the vectors  $\{\mathbf{C}_n \boldsymbol{\theta}_1^{(\ell)}\}_{n=1}^N$  are linearly independent, the matrix  $\sum_{n=1}^N \frac{\alpha_n \delta_n}{M_n} \mathbf{C}_n \boldsymbol{\theta}_1^{(\ell)} \boldsymbol{\theta}_1^{(\ell)\dagger} \mathbf{C}_n^\dagger$  is full rank and  $\lambda_{\min}(\boldsymbol{\theta}_1^{(\ell)})$  is strictly greater than zero. Using (23), it can be seen that, in that case, the denominator of the argument of the Gaussian  $\mathcal{Q}(\cdot)$  function becomes dominated by  $\lambda_{\min}(\boldsymbol{\theta}_1^{(\ell)})$  when the power  $P$  is sufficiently large. Since  $\mathcal{Q}(x) > 0, \forall x$ , it follows that the expectation on the RHS of (23) is strictly greater than zero if there is at least one realization of  $\boldsymbol{\theta}_1^{(\ell)}$  for which  $\lambda_{\min}(\boldsymbol{\theta}_1^{(\ell)}) > 0$ . Hence, we have shown that in the presence of self-interference, the PEP is lower bounded by a strictly positive constant, which implies an error floor and a zero diversity gain. In Section VII, this observation will be confirmed by numerical simulations and in the next section, we will provide a methodology for eliminating this interference perfectly without invoking CSI.

## V. PERFECT SELF-INTERFERENCE CANCELLATION

We have shown that self-interference causes the SINR and the PEP to approach strictly positive constants as  $P \rightarrow \infty$ , thereby implying an error floor and zero diversity gain. Now, we show that the scheme proposed in Section III enables self-interference to be cancelled perfectly, which maximizes the SINR and allows it to go to infinity and the PEP to go to zero as  $P \rightarrow \infty$ .

*Theorem 2:* The average SINR for each node is maximized when the spatial processing matrices in (5) at all the relays,  $\{\mathbf{X}_n\}_{n=1}^N$ , are skew-symmetric.<sup>2</sup>

*Proof:* To find  $\{\mathbf{X}_n\}$  that maximize the SINR, we note that those matrices affect the SINR expression through the nonnegative constants  $\{\alpha_n\}$  in the denominator on the RHS of (22), where  $\{\alpha_n\}_{n=1}^N$  are defined in (20). Hence, the optimal choice of  $\{\mathbf{X}_n\}$  is the one that renders  $\alpha_n = 0, \forall n$ . From (20), it can be seen that this condition can be only satisfied when all the diagonal entries of  $\mathbf{X}_n$  are zero, i.e.,  $x_{kk}^{(n)} = 0$ , and all the off-diagonal entries satisfy  $x_{kl}^{(n)} = -x_{lk}^{(n)}$ , that is, this

<sup>2</sup>Note that cancelling self-interference requires  $\mathbf{X}_n, n = 1, \dots, N$ , to be skew-symmetric, rather than skew-Hermitian.

condition is satisfied if and only if  $\mathbf{X}_n = -\mathbf{X}_n^T$ , which proves the theorem. ■

We have shown that choosing  $\{\mathbf{X}_n\}_{n=1}^N$  to be skew-symmetric maximizes the SINR for all  $P$ . We now show that this choice eliminates self-interference perfectly. From (19) we note that the nonnegative constants  $\{\alpha_n\}$  in (22) are in fact due to self-interference. Hence, enforcing  $\{\alpha_n\}_{n=1}^N$  to be zero is, in effect, the same as eliminating self-interference perfectly. Before discussing other ramifications of choosing  $\{\mathbf{X}_n\}_{n=1}^N$  to be skew-symmetric, we note that eliminating self-interference was made possible by the novel spatial processing proposed in Section III, but could not be effected by previously proposed techniques which restrict the relay received signals to be processed in time only. To elaborate on this observation, we have the following corollary.

*Corollary 1:* Setting the spatial processing matrices,  $\{\mathbf{X}_n\}_{n=1}^N$ , to be skew-symmetric yields  $\mathbf{h}_1 = \mathbf{0}_N$ , i.e., the equivalent channel of self-interference is the all-zero  $N \times 1$  vector.

*Proof:* From (10) and (13) it can be seen that the equivalent channel for the self-interference component is the vector  $\mathbf{h}_1$ . To prove the statement of the corollary, we use  $\gamma_n$  to denote the  $n$ -th entry of  $\mathbf{h}_1$ , i.e.,  $\gamma_n \triangleq \mathbf{f}_n^T \mathbf{X}_n \mathbf{f}_n$ . But since  $\gamma_n$  is a scalar, we must have  $\gamma_n = \gamma_n^T = \mathbf{f}_n^T \mathbf{X}_n^T \mathbf{f}_n = -\mathbf{f}_n^T \mathbf{X}_n \mathbf{f}_n$ , which, together with the definition of  $\gamma_n$ , establishes the claim of the corollary. ■

We have shown that  $\{\mathbf{X}_n\}_{n=1}^N$  must be: 1) unitary for the equivalent channel vectors to be i.i.d. (cf. Section III), and 2) skew-symmetric for self-interference to be perfectly eliminated (cf. Theorem 1 and Corollary 1). Combining these conditions yields:

*Lemma 1:* For the matrix  $\mathbf{X}_n \in \mathbb{C}^{M_n \times M_n}$  to be unitary and skew-symmetric, the dimension  $M_n$  must be even,  $n = 1, \dots, N$ .

*Proof:* To prove this lemma, we note that any skew-symmetric matrix  $\mathbf{X}_n \in \mathbb{C}^{M_n \times M_n}$  satisfies  $|\mathbf{X}_n| = (-1)^{M_n} |\mathbf{X}_n|$ . This implies that when  $M_n$  is odd  $|\mathbf{X}_n| = 0$ . However, for  $\mathbf{X}_n$  to be unitary, the absolute value of  $|\mathbf{X}_n|$  is equal to one. Hence, we conclude that  $M_n$  must be even in order to admit a matrix  $\mathbf{X}_n$  that is both unitary and skew-symmetric. ■

Combining this lemma with Corollary 1 yields that the number of active antennas per relay, must be even to ensure that the equivalent channels are i.i.d. and that self-interference is perfectly eliminated. The following theorem provides the construction that ensures that a square  $\{\mathbf{X}_n\}$  with even dimension is both unitary and skew-symmetric.

*Theorem 3:* Let the eigendecomposition of the unitary matrix  $\mathbf{X}_n$  be given by<sup>3</sup>  $\mathbf{X}_n = \boldsymbol{\Phi}_n \boldsymbol{\Lambda}_n \boldsymbol{\Phi}_n^\dagger$  where  $\boldsymbol{\Lambda}_n \in \mathbb{C}^{2K \times 2K}$ , is diagonal, and  $\boldsymbol{\Phi}_n \in \mathbb{C}^{2K \times 2K}$  is unitary, for some integer  $K$ . Then,  $\mathbf{X}_n$  is skew-symmetric if and only if the diagonal entries of  $\boldsymbol{\Lambda}_n$  are pairwise antipodal and lie on the unit circle, i.e., these entries are given by  $\pm e^{j\theta_k^{(n)}}$ ,  $\theta_k^{(n)} \in [0, 2\pi)$ ,  $k = 1, \dots, K$ , and the columns of  $\boldsymbol{\Phi}_n$  are pairwise conju-

<sup>3</sup>This decomposition exists because  $\mathbf{X}_n$  is unitary and hence normal [24].

gates, i.e.,  $\Phi_n$  is given by  $\Phi_n = [\phi_1^{(n)}, \bar{\phi}_1^{(n)}, \dots, \phi_K^{(n)}, \bar{\phi}_K^{(n)}]$ . Furthermore, such a unitary matrix  $\Phi_n$  can be constructed from an arbitrary real orthogonal matrix  $\mathbf{Q}_n = [\mathbf{q}_1^{(n)}, \mathbf{q}_2^{(n)}, \dots, \mathbf{q}_{2K}^{(n)}] \in \mathbb{R}^{2K \times 2K}$  using  $\phi_k^{(n)} = \frac{1}{\sqrt{2}}(\mathbf{q}_{2k-1}^{(n)} + j\mathbf{q}_{2k}^{(n)})$ ,  $k = 1, \dots, K$ .

*Proof:* See Appendix C.  $\blacksquare$

The result reported in this theorem renders the construction of general unitary skew-symmetric spatial processing matrices straightforward. In the next section we will investigate the effect of using such matrices on the PEP attained by the TWRN under consideration.

## VI. PERFORMANCE ANALYSIS UNDER PERFECT SELF-INTERFERENCE CANCELLATION

### A. Asymptotically Optimal Channel-Unaware

#### Symbol Detection

So far, it is shown that choosing  $\{\mathbf{X}_n\}_{n=1}^N$  in (5) to be skew-symmetric when the number of active antennas at the relays is even leads to perfect self-interference cancellation. Hence, the received signal of node 1 in (10) can be expressed as

$$\mathbf{y}_1^{(\ell)} = \sqrt{P_2} \mathbf{S}_2^{(\ell)} \mathbf{h}_2 + \mathbf{w}_1^{(\ell)}. \quad (24)$$

Although (24) is valid only when self-interference is cancelled perfectly, it is sometimes used to approximate the received signal when self-interference is partially cancelled [15], [16]. This approximation maybe somewhat misleading. Indeed, Section IV shows that residual self-interference can cause serious SINR and PEP degradation, and results in zero diversity and error floor.

To analyze performance when self-interference is cancelled perfectly, we use (1) and (9) to write  $\mathbf{C}_n \theta_i^{(\ell)}$ , the  $n$ -th column of  $\mathbf{S}_i^{(\ell)}$  (cf. (11)), as  $\mathbf{U}_i \mathbf{C}_n \theta_i^{(\ell-1)}$  [7], [16]. Hence, we have

$$\mathbf{S}_i^{(\ell)} = \left[ \mathbf{U}_i^{(\ell)} \mathbf{C}_1 \theta_i^{(\ell-1)} \dots \mathbf{U}_i^{(\ell)} \mathbf{C}_N \theta_i^{(\ell-1)} \right] = \mathbf{U}_i^{(\ell)} \mathbf{S}_i^{(\ell-1)}.$$

Using this in (24), the received signal of node 1 during the  $\ell$ -th block can be represented as

$$\mathbf{y}_1^{(\ell)} = \mathbf{U}_2^{(\ell)} \mathbf{y}_1^{(\ell-1)} + \mathbf{w}_1^{(\ell)} - \mathbf{U}_2^{(\ell)} \mathbf{w}_1^{(\ell-1)}. \quad (25)$$

For close to maximum likelihood (ML) detection, the distribution of  $\mathbf{w}_1^{(\ell)}$  is assumed to be Gaussian (cf. Section III), yielding the following ML detector [7], [16]:

$$\arg \min_{\mathbf{U}_2} \left\| \Sigma_{\mathbf{w}_1}^{-\frac{1}{2}} (\mathbf{y}_1^{(\ell)} - \mathbf{U}_2^{(\ell)} \mathbf{y}_1^{(\ell-1)}) \right\|^2, \quad (26)$$

where  $\Sigma_{\mathbf{w}_1}$  is given in (15). The detector in (26) is channel-unaware because it is not a function of  $\mathbf{f}_n$  and  $\mathbf{g}_n$ . An upper bound on the PEP achieved by this detector is derived next.

### B. An Upper Bound on the PEP

The following theorem gives an upper bound on the PEP when self-interference is cancelled perfectly and the ML symbol detector (26) is used.

*Theorem 4:* When  $\{\mathbf{X}_n\}_{n=1}^N$  are unitary skew-symmetric matrices, the high-power PEP satisfies

$$\Pr(\mathbf{S}_{2,a}^{(\ell)} \rightarrow \mathbf{S}_{2,b}^{(\ell)}) \leq \left( P G_c(\mathbf{S}_{2,a}^{(\ell)}, \mathbf{S}_{2,b}^{(\ell)}) \right)^{-G_d}, \quad (27)$$

where  $G_d$ , the diversity gain, and  $G_c$ , the coding gain, are respectively given by

$$\begin{aligned} G_d &= N, \\ G_c(\mathbf{S}_{2,a}^{(\ell)}, \mathbf{S}_{2,b}^{(\ell)}) &= \frac{\delta_0}{16} |(\mathbf{S}_{2,a}^{(\ell)} - \mathbf{S}_{2,b}^{(\ell)})^\dagger (\mathbf{S}_{2,a}^{(\ell)} - \mathbf{S}_{2,b}^{(\ell)})|^{\frac{1}{N}} g_c(M_n)^{-\frac{1}{N}}, \\ g_c(M_n) &\triangleq \frac{(1 + \delta_0 + N \sum_{n=1}^N \delta_n)^N \Pr(\|\mathbf{f}_n\|^2 \leq M_n)}{\prod_{n=1}^N \delta_n} \\ &\quad + \frac{(1 + \delta_0)^N + N^N \sum_{n=1}^N (\frac{\delta_n}{M_n})^N \frac{(N+M_n-1)!}{(M_n-1)!}}{\prod_{n=1}^N \delta_n} \\ &\quad \times \Pr(\|\mathbf{f}_n\|^2 > M_n). \end{aligned} \quad (28)$$

*Proof:* See Appendix D.  $\blacksquare$

First, this theorem shows that the diversity gain characterizes the rate at which the PEP decays with  $P$  and that the coding gain does not involve  $P$ . Hence, that slope of PEP, and subsequently the union bound is determined by  $N$ , the number of relays, and does not depend on the number of antennas at the relays,  $\{M_n\}_{n=1}^N$ . The reason for which the diversity gain is independent of the number of antennas at the relays is due to the fact that the diversity gain is determined by the number of linear transformations of the transmitted signals received at the destination. Using (11), it can be seen that, irrespective of the number of antennas, each relay generates one linear transformation of the transmitted signal at the destination node, i.e., one column of the received matrix, leading to a diversity gain equal to the number of relays. Second, the coding gain increases with  $M_n$  and converges to a constant at  $M_n \rightarrow \infty$ . To elaborate, we show that  $g_c(M_n + 2) - g_c(M_n)$  is negative and converges to 0 at  $M_n \rightarrow \infty$ . For ease of exposition, we assume that all relays and both nodes use the same power, i.e.,  $\{\delta_n\}_{n=0}^N = 1$ , and that all relays have the same number of antennas, i.e.,  $M_n = M$ ,  $\forall n$ . Using these assumptions in (29) along with the fact that, for large  $M$ ,  $\frac{N^{N+1}(N+M+1)!}{(M+2)^N(N+M+1)!} \approx \frac{N^{N+1}(N+M-1)!}{M^N(M-1)!} \approx N^{N+1}$ , yields  $g_c(M+2) - g_c(M) = ((2 + N^2)^N - 2^N - N^{N+1})(\Pr(\|\mathbf{f}_n\|^2 \leq M+2) - \Pr(\|\mathbf{f}_n\|^2 \leq M))$ . Using the cumulative probability function (CDF) of  $\|\mathbf{f}_n\|^2$  in (63) in Appendix D, it can be shown that, for large  $M$ ,  $\Pr(\|\mathbf{f}_n\|^2 \leq M+2) - \Pr(\|\mathbf{f}_n\|^2 \leq M) \nearrow 0$ , i.e., for any large but finite  $M$ ,  $\Pr(\|\mathbf{f}_n\|^2 \leq M+2) - \Pr(\|\mathbf{f}_n\|^2 \leq M) < 0$  and approaches 0 as  $M \rightarrow \infty$ . This confirms that  $G_c$  increases with  $M$  and converges to a constant as  $M \rightarrow \infty$ . Since high-power performance is dominated by the diversity gain [2], the aforementioned results yield that increasing the number of relays is more beneficial than increasing the number of antennas per relay.

Using (27), we obtain the union bound on the average block error rate (BLER) at high powers. To do so, let  $P_e(\mathbf{S}_{2,a}^{(\ell)})$  be the probability that node 2 sends the message  $\mathbf{S}_{2,a}^{(\ell)}$  during the  $\ell$ -th block and node 1 makes an error in detecting it. A standard argument asserts that  $P_e(\mathbf{S}_{2,a}^{(\ell)}) \leq \sum_{b=1, b \neq a}^{\Upsilon} \Pr(\mathbf{S}_{2,a}^{(\ell)} \rightarrow \mathbf{S}_{2,b}^{(\ell)})$ , where  $\Upsilon$  denotes the cardinality of  $\{\mathbf{S}_{2,a}^{(\ell)}\}$ . For equiprobable messages,  $\text{BLER} = \frac{1}{\Upsilon} \sum_{a=1}^{\Upsilon} P_e(\mathbf{S}_{2,a}^{(\ell)})$  and the bound on

$P_e(\mathbf{S}_{2,a}^{(\ell)})$  and (27) yield

$$\text{BLER} \leq \frac{1}{\Upsilon} P^{-G_d} \sum_{a=1}^{\Upsilon} \sum_{b=1, b \neq a}^{\Upsilon} G_c(\mathbf{S}_{2,a}^{(\ell)}, \mathbf{S}_{2,b}^{(\ell)})^{-G_d}. \quad (30)$$

Although the union bound is commonly used in the literature [16], [25], [26], it is generally loose because of the Chernoff bound on the  $Q(\cdot)$  function in the derivation of (27) and the number of terms in the summation [27]. Finding a tighter bound seems difficult, and even if such a bound were to be found, it may not yield insight into the key elements that govern performance. In contrast, examining the bound in (30) reveals that the terms in the summation do not depend on  $P$ , which implies that at high  $P$ , it will have approximately the same slope as the actual BLER, but with a gap that increases with  $\Upsilon$ . This observation will be confirmed in Section VII.

### C. Computational Complexity Analysis

Using (5), it can be seen that the complexity of the proposed signalling scheme is dominated by the multiplication of  $\mathbf{C}_n$ ,  $\mathbf{R}_n^{(\ell)}$  and  $\mathbf{X}_n$ . Hence the number of multiplications in this scheme is  $O(\sum_{n=1}^N (N^2 M_n + N M_n^2))$ . However, Theorem 4 and the results in Section VII below suggest choosing  $M_n$  to be even and relatively small, e.g.,  $M_n = 4$ ,  $\forall n$ . In this case, the number of multiplications of our scheme is  $O(4N^3 + 16N^2)$ . In contrast, the scheme in [16] relies on blind channel estimation prior to interference cancellation. Hence in that scheme, processing at the relays, channel estimation and subsequent self-interference cancellation require  $O(N^3 + LN^2)$  multiplications, where  $L \geq 2N$ . Hence, the asymptotic computational complexity of both schemes grows cubically with  $N$ , but our scheme is able to cancel self-interference perfectly.

## VII. SIMULATION

In this section, we compare the performance of the scheme proposed herein with that of the one proposed in [16] for various DDST codes, including the (linear)  $2 \times 2$  and  $4 \times 4$  real orthogonal codes [4], [7]<sup>4</sup> and the (sesquilinear) Alamouti [7], [28], and  $SP(2)$  [7], [29] codes. For all examples, the skew-symmetric unitary matrices are chosen to be  $\mathbf{X}_n = \bigoplus_{k=1}^{M_n/2} \mathbf{J}$  (cf. (8)), the entries of  $\{\mathbf{f}_n\}$ ,  $\{\mathbf{g}_n\}$ ,  $\{\mathbf{V}_n^{(\ell)}\}$  and  $\{\mathbf{z}_i^{(\ell)}\}$  are zero mean Gaussian with unit variance. For ease of exposition, we will assume that both nodes and all relays use equal transmit powers, i.e.,  $\delta_0 = \delta_n = 1$ , and equal number of antennas, i.e.,  $M_n = M$ ,  $n = 1, \dots, N$ , where  $M$  is taken to be even, cf. Lemma 1. Without loss of generality, we will set the initialization vector  $\mathbf{s}_i^{(0)} = [1 \dots 1]^T$ ,  $i = 1, 2$ , and for the examples with block fading channels, we will use the coherence time considered in [16], i.e.,  $T = 100$ .

<sup>4</sup>We were unable to simulate the case with  $8 \times 8$  real orthogonal codes because the relay matrices  $\{\mathbf{A}_n\}$  and the corresponding unitary differential coding matrices  $\{\mathbf{U}_i^{(\ell)}\}$  provided in [7] do not satisfy the commuting property in (9).

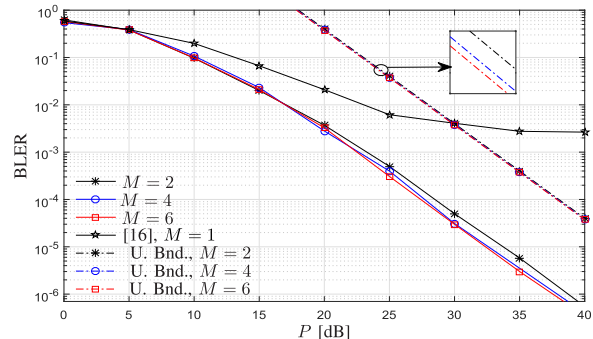


Fig. 2.  $N = 2$  relays and  $2 \times 2$  real orthogonal code.

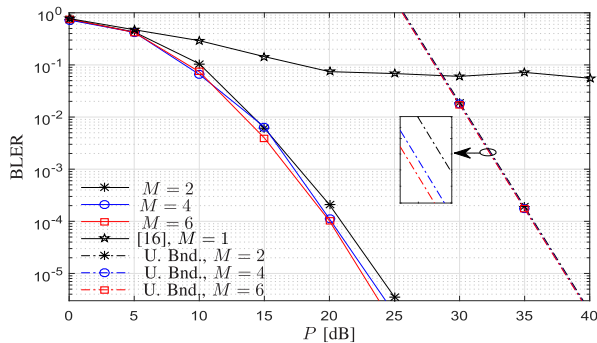
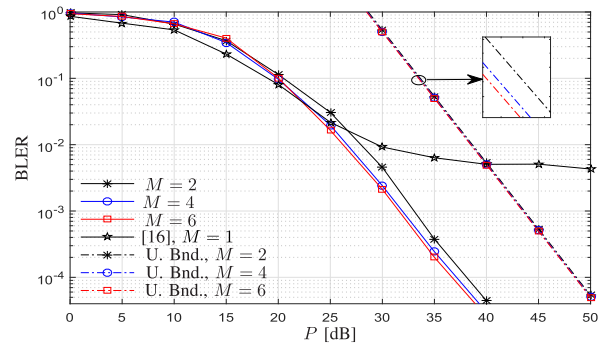
### A. Block Error Rate Performance

In this section we compare the BLER performance of the scheme proposed herein and the one proposed in [16] for various DDST codes.

*Example 1:* In this example, we consider a TWRN with  $N = 2$  relays using the (linear)  $2 \times 2$  real orthogonal code in [4] and [7]. Using this code, the time domain relay matrices  $\{\mathbf{C}_n\}$  in (7) are  $\mathbf{C}_1 = \mathbf{I}_2$  and  $\mathbf{C}_2 = \mathbf{J}$ , and the unitary matrices in (1) are  $\mathbf{U}_i^{(\ell)} = \begin{bmatrix} u_1^{(\ell)} & -u_2^{(\ell)} \\ u_2^{(\ell)} & u_1^{(\ell)} \end{bmatrix}$ , where  $\{u_r^{(\ell)}\}$  is selected from the pulse amplitude modulation (PAM) constellation. Note that these matrices and the corresponding ones in the forthcoming examples satisfy the commuting property in (9). For this example, we use the 2-PAM constellation which results in an overall data rate of 1 bit per channel use (bpcu), i.e., 0.5 bpcu from node  $i$  to node  $j$ ,  $i \neq j$ .

For comparison, the BLER performance and the union bound (U. Bnd. in the figures) in (30) for the proposed DDST code are depicted in Figure 2 for the cases of  $M = 2$ , 4 and 6 antennas per relay. The high-power diversity gain of the proposed scheme can be deduced from Figure 2 by numerical evaluation of the gradient of the BLER curves. Taking the coordinates of two points in the high-power region of the curve, e.g.,  $(P_a, \text{BLER}_a)$  and  $(P_b, \text{BLER}_b)$ , the numerically evaluated diversity gain can be expressed as  $\tilde{G}_d = \frac{\log(\text{BLER}_a) - \log(\text{BLER}_b)}{\log(P_a) - \log(P_b)}$ . Performing this computation for the scenario in Figure 2 yields  $\tilde{G}_d = 1.95$ , which is close to the diversity gain predicted by (28), namely,  $G_d = 2$ . Note, that as predicted by (28),  $G_d$  is determined by the numbers of relays,  $N$ , but not the number of antennas per relay,  $M$ , provided that  $M \geq 2$ . This is in contrast with the scheme in [16], whose performance is also depicted in Figure 2. In that scheme, each relay has one antenna, i.e.,  $M = 1$ , which prevents the relays from spatial processing of their received signals and results in imperfect self-interference cancellation and zero high-power diversity order, cf. Theorem 1. Furthermore, Figure 2 confirms Theorem 4, which predicts that the coding gain in (29) increases and converges to a constant as  $M$  increases, cf. zoomed bounds.  $\square$

*Example 2:* The setup for this example resembles the one for Example 1 except with  $N = 4$  relays. The linearly-structured DDST code herein is the  $4 \times 4$  real orthogonal code

Fig. 3.  $N = 4$  relays and  $4 \times 4$  real orthogonal code.Fig. 4.  $N = 2$  relays and  $2 \times 2$  Alamouti code.

with the following time relay processing and constellation matrices [4], [7]:  $A_1 = I_4$ ,  $A_2 = \bigoplus_{k=1}^2 J$ ,

$$A_3 = \begin{bmatrix} 0 & 0 & -1 & 0 \\ 0 & 0 & 0 & 1 \\ 1 & 0 & 0 & 0 \\ 0 & -1 & 0 & 0 \end{bmatrix}, \quad A_4 = \begin{bmatrix} 0 & 0 & 0 & -1 \\ 0 & 0 & -1 & 0 \\ 0 & 1 & 0 & 0 \\ 1 & 0 & 0 & 0 \end{bmatrix},$$

$$\text{and } U_i^{(\ell)} = \begin{bmatrix} u_1^{(\ell)} & -u_2^{(\ell)} & -u_3^{(\ell)} & -u_4^{(\ell)} \\ u_2^{(\ell)} & u_1^{(\ell)} & u_4^{(\ell)} & -u_3^{(\ell)} \\ u_3^{(\ell)} & -u_4^{(\ell)} & u_1^{(\ell)} & u_2^{(\ell)} \\ u_4^{(\ell)} & u_3^{(\ell)} & -u_2^{(\ell)} & u_1^{(\ell)} \end{bmatrix}.$$

These matrices satisfy the commuting property in (9) and, in this example, the entries of  $\{U_i^{(\ell)}\}$ ,  $\{u_r^{(\ell)}\}$ , are chosen from the 2-PAM constellation, yielding an overall rate of 1 bpcu.

The performance of the proposed scheme and the one in [16] are depicted in Figure 3. From this figure, the numerically evaluated diversity gain at moderate powers, e.g.,  $P = 25$  dB, is  $\tilde{G}_d = 3.59$  while the analytically predicted diversity gain is  $G_d = 4$ . This discrepancy is because, in Figure 3,  $P$  is not sufficiently high for the diversity gain to dominate performance. Figure 3 also shows that the scheme in [16] does not have a diversity gain and produces an error floor at powers beyond 25 dB. This figure, also shows that, similar to the case in Example 1, the coding gain converges to a constant, which agrees with the analytical results in Section VI-B.  $\square$

*Example 3:* In this example, we consider a TWRN with  $N = 2$  relays using the (sesquilinear) DDST Alamouti code [28], [7]. For this code the matrices,  $\{C_n\}$  in (7), are constructed with  $A_1 = I_2$ ,  $B_1 = \mathbf{0}$ ,  $A_2 = \mathbf{0}$ , and  $B_2 = J$ , and the unitary differential encoding matrices are given by  $U_i^{(\ell)} = \frac{1}{\sqrt{|u_1^{(\ell)}|^2 + |u_2^{(\ell)}|^2}} \begin{bmatrix} u_1^{(\ell)} & -\bar{u}_2^{(\ell)} \\ u_2^{(\ell)} & \bar{u}_1^{(\ell)} \end{bmatrix}$ , where  $u_1^{(\ell)}$  and  $u_2^{(\ell)}$ , are selected from any complex constellation, e.g., phase shift keying (PSK) and quadrature amplitude modulation (QAM) ones.

The signalling scheme proposed herein requires  $3N$  time slots, whereas, the scheme proposed in [16] requires  $2N$  times slots. Hence, for fair comparison, for the scheme proposed herein we will choose  $u_1^{(\ell)}$  and  $u_2^{(\ell)}$  in  $U_i^{(\ell)}$  from the 8-PSK constellations and for the one proposed in [16], we will choose  $u_1^{(\ell)}$  and  $u_2^{(\ell)}$  in  $U_i^{(\ell)}$  from the 4-PSK constellations. These

constellations ensure that both schemes operate at an overall data rate of 2 bpcu.

The performance of the proposed scheme and the one in [16] are shown in Figure 4. From this figure, it can be seen the scheme proposed in [16] exhibits better performance at low powers. For instance at a BLER of  $10^{-1}$ , the performance advantage of the scheme in [16] is about 1 dB. However, at higher powers, the scheme proposed herein significantly outperforms the one in [16]. In particular, the BLER yielded by the scheme in [16] flattens out at  $6 \times 10^{-3}$ , whereas the BLER of our scheme continues to decay with  $P$  with a diversity gain approximately equal to the number of relays, i.e., 2. Similar to the linear cases considered in Examples 1 and 2, increasing  $M$  leads the coding gain to converge to a constant, as predicted in Section IV-B.  $\square$

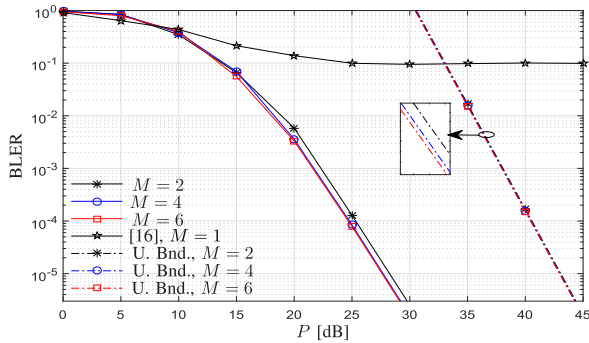
*Example 4:* The setup for this example resembles the one for Example 3 except with  $N = 4$  relays. In this case the the sesquilinear code is  $4 \times 4$   $SP(2)$  with the following time processing and constellation matrices [7], [29]:  $A_1 = I_4$ ,  $B_1 = B_4 = \mathbf{0}$ ,  $A_2 = A_3 = \mathbf{0}$ ,  $B_2 = \bigoplus_{k=1}^2 J$ ,

$$B_3 = \begin{bmatrix} 0 & 0 & -1 & 0 \\ 0 & 0 & 0 & -1 \\ 1 & 0 & 0 & 0 \\ 0 & 1 & 0 & 0 \end{bmatrix}, \quad A_4 = \begin{bmatrix} 0 & 0 & 0 & 1 \\ 0 & 0 & -1 & 0 \\ 0 & -1 & 0 & 0 \\ 1 & 0 & 0 & 0 \end{bmatrix},$$

$$\text{and } U_i^{(\ell)} = \begin{bmatrix} u_1^{(\ell)} & -\bar{u}_2^{(\ell)} & -\bar{u}_3^{(\ell)} & u_4^{(\ell)} \\ u_2^{(\ell)} & \bar{u}_1^{(\ell)} & -\bar{u}_4^{(\ell)} & -u_3^{(\ell)} \\ u_3^{(\ell)} & -\bar{u}_4^{(\ell)} & \bar{u}_1^{(\ell)} & -u_2^{(\ell)} \\ u_4^{(\ell)} & \bar{u}_3^{(\ell)} & \bar{u}_2^{(\ell)} & u_1^{(\ell)} \end{bmatrix}.$$

These matrices satisfy the commuting property in (9) and,  $u_1^{(\ell)} = \frac{a_1^{(\ell)} a_2^{(\ell)} - b_1^{(\ell)} \bar{b}_2^{(\ell)}}{\sqrt{2} \prod_{k=1}^2 \sqrt{|a_k^{(\ell)}|^2 + |b_k^{(\ell)}|^2}}$ ,  $u_2^{(\ell)} = -\frac{\bar{a}_1^{(\ell)} \bar{b}_2^{(\ell)} + b_1^{(\ell)} a_2^{(\ell)}}{\sqrt{2} \prod_{k=1}^2 \sqrt{|a_k^{(\ell)}|^2 + |b_k^{(\ell)}|^2}}$ ,  $u_3^{(\ell)} = -\frac{\bar{a}_1^{(\ell)} a_2^{(\ell)} - \bar{b}_1^{(\ell)} \bar{b}_2^{(\ell)}}{\sqrt{2} \prod_{k=1}^2 \sqrt{|a_k^{(\ell)}|^2 + |b_k^{(\ell)}|^2}}$ , and  $u_4^{(\ell)} = \frac{a_1^{(\ell)} \bar{b}_2^{(\ell)} + b_1^{(\ell)} a_2^{(\ell)}}{\sqrt{2} \prod_{k=1}^2 \sqrt{|a_k^{(\ell)}|^2 + |b_k^{(\ell)}|^2}}$ ,  $a_k^{(\ell)} \in \mathbb{F}_k$ ,  $b_k^{(\ell)} \in \mathbb{G}_k$ ,  $k = 1, 2$ , and  $\mathbb{F}_k$  and  $\mathbb{G}_k$  are PSK sets.

To obtain a rate for our scheme that is close to a rate supported by the scheme in [16], in our scheme, we choose  $a_1^{(\ell)}$  and  $b_1^{(\ell)}$  from the 5-PSK constellation and  $a_2^{(\ell)}$  and  $b_2^{(\ell)}$  from the 3-PSK constellation, yielding an overall data rate

Fig. 5.  $N = 4$  relays and  $4 \times 4$   $SP(2)$  code.

of 1.2925 bpcu. For the scheme in [16],  $a_1^{(\ell)}$  and  $b_1^{(\ell)}$  are chosen from the 2-PSK constellation and  $a_2^{(\ell)}$  and  $b_2^{(\ell)}$  are chosen from the 3-PSK constellations, yielding an overall data rate of 1.3023 bpcu.

In Figure 5, we depict the performance of the scheme proposed herein with the one in [16] along with the union bound in (30). As in the previous examples, Figure 5 confirms that the high-power diversity gain of the proposed scheme is  $N = 4$  and the coding gain converges to a constant with the increase of the number of relay antennas,  $M$ .  $\square$

In the previous examples, the performance of the proposed scheme and the one in [16] were compared when both schemes used the same DDST code, i.e., the same number of relays. Since in the proposed scheme each relay uses an even number of antennas, whereas in the scheme in [16] each relay uses one antenna, the total number of antennas at the relays is not equal for the two schemes. Comparing the performance of these schemes when they use the same total number of relay antennas can be insightful. Such a comparison is provided in the next example.

*Example 5:* In this example, we compare the schemes proposed herein and in [16] when each uses a total of 4 antennas at the relays for both linear and sesquilinear codes. Since the proposed scheme uses an even number of antennas and [16] uses one antenna per relay, we consider two relays with two antennas each in the proposed scheme and four single-antenna relays in [16]. For  $N = 2$  relays, the proposed scheme uses the  $2 \times 2$  real orthogonal and the Alamouti codes for the linear and sesquilinear codes, respectively. The corresponding codes for the scheme in [16] when  $N = 4$  relays are the  $4 \times 4$  real orthogonal and the  $SP(2)$  codes, respectively. For fair comparison, in the case of linear codes, we use 2-PAM constellation for both the  $2 \times 2$  and  $4 \times 4$  real orthogonal codes, resulting in an overall data rate of 1 bpcu. For sesquilinear codes, we use 4-PSK for the Alamouti code which results in a data rate of 1.33 bpcu and we use 2-PSK for  $a_1^{(\ell)}$  and  $b_1^{(\ell)}$  and 3-PSK for  $a_2^{(\ell)}$  and  $b_2^{(\ell)}$  for the  $SP(2)$  code which results in a data rate of 1.29 bpcu. Similar to the previous cases, Figure 6 confirms that perfect self-interference cancellation enables the proposed scheme to significantly outperform the one in [16].  $\square$

In the previous examples, the channels were assumed to be block fading, whereby the fading coefficients remain constant throughout the coherence time  $T$ . However, in many scenarios,

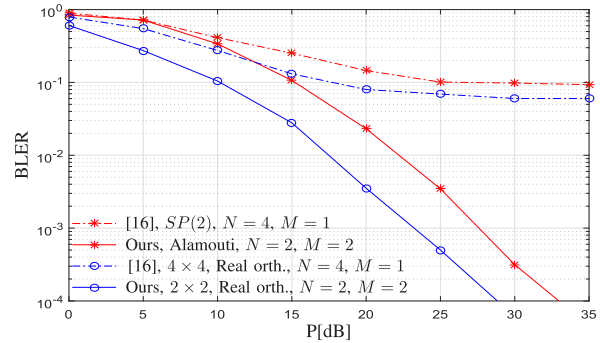
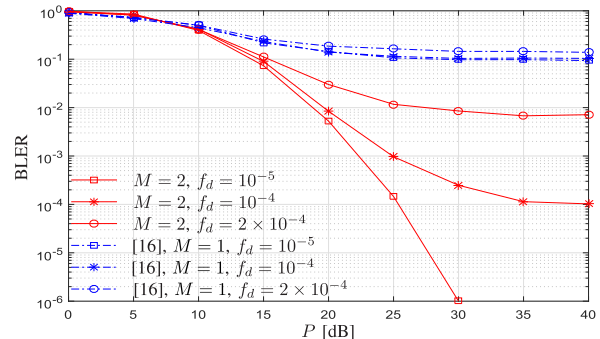


Fig. 6. Performance comparison when the total number of relay antennas is equal to 4.

Fig. 7. Jakes' fading channels with various  $f_d$ .

the channels undergo continuous temporal variations, which are usually captured by various statistical models including the Jakes' fading one [30]. In this model the correlation parameters that characterize the channel variations depend on the mobility of the nodes and/or the relays. To elaborate, let  $f[k]$  be a fading coefficient at time  $k$ . Then, in Jakes' model, the autocorrelation of this coefficient is  $E\{f[k]\bar{f}[k+k_0]\} = J_0(4\pi k_0 f_d)$ , where  $J_0(\cdot)$  is the zeroth-order Bessel function of the first kind, and  $f_d$  is the maximum normalized Doppler frequency of the channel.

We now examine the scheme proposed herein and the one in [16] in Jake's fading channels.

*Example 6:* The set up in this example resembles the one in Example 4 but with Jakes' fading channels and  $M = 2$  antennas for each of the 4 relays. For simplicity, all channel coefficients are assumed to have the same  $f_d$ . The BLER performance comparison is provided in Figure 7 for  $f_d = 10^{-5}$ ,  $10^{-4}$  and  $2 \times 10^{-4}$ . From this figure, it can be seen that at  $f_d = 10^{-5}$ , the BLER corresponding to scheme proposed herein continues to decay with  $P$ , whereas that corresponding to the scheme in [16] exhibits an error floor at  $P = 20$  dB. For instance, at  $f_d = 10^{-5}$  and  $P = 30$  dB, the scheme in [16] yields a BLER of  $10^{-1}$ , whereas our scheme yields a BLER of  $10^{-6}$ . Increasing  $f_d$  to  $10^{-4}$ , the scheme proposed herein and the one in [16] begin to exhibit an error floor at about  $P = 35$  dB and  $P = 20$  dB, respectively, but the scheme proposed herein exhibits a significantly lower BLER;  $10^{-4}$  for our scheme versus  $10^{-1}$  for the one in [16].  $\square$

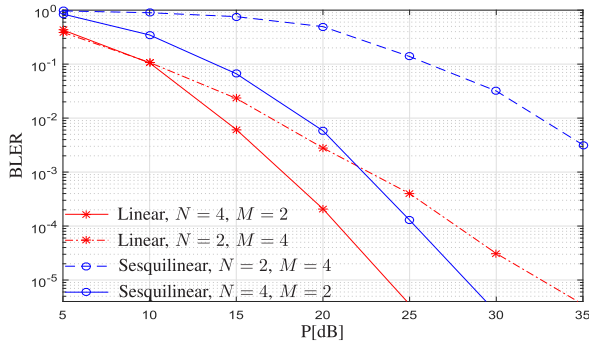


Fig. 8. Effect of distributing antennas over more relays.

### B. Effect of Number of Relays and Number of Antennas per Relay

In Section VI-B we showed that increasing the number of relays is more beneficial than increasing the number of antennas per relay. Herein, we further investigate this analytical finding. We consider a total of 8 antennas at the relays and two different cases. In the first case, we assume that there are  $N = 2$  relays, each with  $M = 4$  antennas, whereas in the second case we assume that there are  $N = 4$  relays, each with  $M = 2$  antennas. The BLERs corresponding to both cases for linear and sesquilinear codes are shown in Figure 8. From this figure it can be seen that, for both classes of codes, the setup with  $N = 4$  relays yields significantly lower BLERs. For instance, at a BLER of  $10^{-4}$ , the case with  $N = 4$  and sesquilinear codes has an advantage of 7 dB over its counterpart with  $N = 2$ . This figure also shows that the rate of BLER decay is doubled when the number of relays is increased from  $N = 2$  to  $N = 4$ . This confirms that the diversity gain depends only on the number of relays as predicted by Theorem 4.

### C. SINR Performance

In this section, we numerically evaluate the average SINR corresponding to the scheme proposed herein and the one proposed in [16] when both schemes use Alamouti code with the setup in Example 3. The simulation results are depicted in Figure 9. This figure shows that as  $P$  increases, the perfect self-interference cancellation of the scheme proposed herein causes the SINR to exhibit linear unbounded increase. In contrast, imperfect cancellation of self-interference in the scheme in [16] causes the corresponding SINR to saturate. These numerical results conform to the analytical SINR expression in (22). Indeed, this expression predicts that perfect self-interference cancellation will yield  $\{\alpha_n\}_{n=1}^N = 0$ , which further implies that the number of antennas per relay does not contribute to the SINR expression as confirmed in Figure 9.

### D. Rate Performance

In Section II, we showed that, for sesquilinear codes, the schemes proposed herein and in [16] consume  $3N$  and  $2N$  symbol durations, respectively. This difference induces a trade-off between the transmission rate per block and perfect

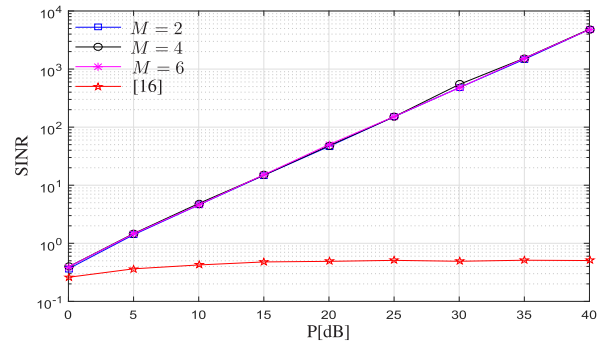


Fig. 9. SINR performance.

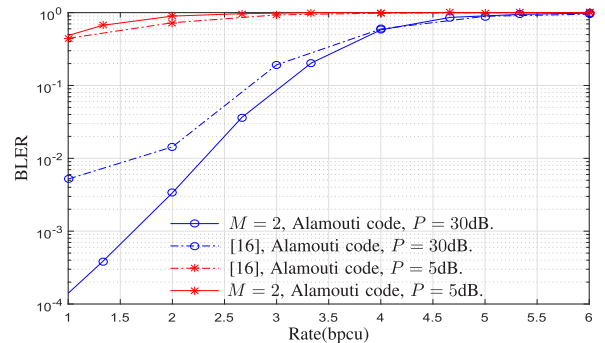


Fig. 10. Rate performance.

self-interference cancellation.<sup>5</sup> Hence, to operate at the same rate, if the cardinality of the constellation used in [16] is  $\Lambda$ , that of the constellation used in the scheme proposed herein must be  $\Lambda^{3/2}$ . To explore the trade-off invoked by this difference, we numerically evaluate the average BLER versus the transmission rate per block when both schemes use Alamouti code at  $P = 5$  and  $P = 30$  dB. This comparison is depicted in Figure 10, which shows that, at  $P = 5$  dB, the scheme in [16] performs slightly better. This is because, at low powers, the impact of self-interference is not large and the BLER is dominated by the constellation size. In contrast, at  $P = 30$ , our proposed scheme exhibits better performance. This is because at high powers, if self-interference is not cancelled, its impact dominates the BLER.

## VIII. SUMMARY

The differences between the proposed scheme and the one in [16] are summarized in Table I. The scheme proposed herein cancels the self-interference perfectly without estimating the channel whereas the scheme proposed in [16] uses blind estimates of the channel to cancel self-interference. Under the assumption that the channel can be perfectly estimated, the analysis of the scheme in [16] shows that it achieves an asymptotic diversity gain equal to the number of relays. However, this assumption is particularly critical because acquiring accurate estimates require the channel to remain constant for a long time, which may not be the case in many practical scenarios. Theorem 1 herein asserts that imperfect estimation of

<sup>5</sup>This trade-off does not exist in the case of linear codes, because in that case both schemes consume  $2N$  symbol durations.

TABLE I  
COMPARISON OF THE SCHEME PROPOSED HEREIN AND [16]

	Scheme proposed in [16]	Scheme proposed herein
Transmitted signal at node $i$	$\mathbf{s}_i^{(\ell)}$	$\mathbf{s}_i^{(\ell)} / [\mathbf{s}_i^{(\ell)T}, \bar{\mathbf{s}}_i^{(\ell)T}]^T$ , linear/sesquilinear codes
Block transmission duration	$2N$	$2N/3N$ , linear/sesquilinear codes
TWRN rate, $\Lambda$ :constellation size	$\log_2 \Lambda$	$\log_2 \Lambda / \frac{2}{3} \log_2 \Lambda$ , linear/sesquilinear codes
Relay processing	Time domain [16]: $\mathbf{t}_n^{(\ell)} = \beta_n (\mathbf{A}_n \mathbf{r}_n^{(\ell)} + \mathbf{B}_n \bar{\mathbf{r}}_n^{(\ell)})$	Time-space domain (cf. (5)): $\mathbf{T}_n^{(\ell)} = \beta_n \mathbf{C}_n \mathbf{R}_n^{(\ell)} \mathbf{X}_n$
Self-interference cancellation	Step 1: Blind channel estimation [16]: $\mathbf{h}_2^{(\ell)} = \frac{\sum_{l=1}^L \mathbf{S}_2^{(\ell-l)\dagger} \mathbf{y}_2^{(\ell-l)}}{NL\sqrt{P_2}}$ , Step 2: Non-perfect cancellation [16]: $\hat{\mathbf{y}}_2^{(\ell)} = \mathbf{y}_2^{(\ell)} - \sqrt{P_2} \mathbf{S}_2^{(\ell)} \mathbf{h}_2^{(\ell)}$ .	Perfect cancellation by skew-symmetric $\mathbf{X}_n$ , $\forall n$ (cf. Section V)
Diversity gain	0 (cf. Section IV-B)	$N$ (cf. (28))
Complexity order	$\mathcal{O}(N^3 + LN^2)$ (cf. Section VI-C)	$\mathcal{O}(\sum_{n=1}^N (N^2 M_n + N M_n^2))$ (cf. Section VI-C)
SINR at $P \rightarrow \infty$	A finite constant (cf. Section IV-A)	$\infty$ (cf. Section IV-A)

the channel will result in residual self-interference, which will subsequently result in an error floor and a zero diversity.

## IX. CONCLUSION

In this paper we proposed a novel signalling scheme for TWRNs in which two single-antenna nodes exchange information via multiple two-way relays, each with multiple antennas. Neither the relays nor the nodes have access to CSI. Unlike existing DDST methods, e.g., the scheme in [16], the novel signalling scheme proposed herein uses joint space-time processing of the relay received signals to eliminate self-interference perfectly at both nodes. We showed that perfect elimination of self-interference requires the space-domain relay processing matrices to be skew-symmetric and unitary, thereby implying that the number of active antennas at each relay must be even. Analyzing the effect of self-interference on the SINR and the PEP, we showed that, unless perfectly cancelled, residual self-interference will result in a zero diversity gain and an asymptotic error floor. Furthermore, we showed that using the scheme proposed herein enables a high-power diversity gain equal to the number of relays to be achieved, irrespective of the number of antennas per relay. Furthermore, we showed that the coding gain of the system increases and converges to a constant as the number of antennas per relay increases.

## APPENDIX A

### PROOF OF (15), (18) AND (19)

#### A. Proof of (15)

Using the statistical independence of  $\{\mathbf{f}_n\}_{n=1}^N$ ,  $\{\mathbf{V}_n^{(\ell)}\}_{n=1}^N$  and  $\mathbf{z}_1^{(\ell)}$  in (14), we write

$$\begin{aligned} \mathbb{E}\{\mathbf{w}_1^{(\ell)} \mathbf{w}_1^{(\ell)\dagger}\} &= \mathbb{E}\left\{\sum_{n=1}^N \beta_n^2 \mathbf{C}_n \mathbf{V}_n^{(\ell)} \mathbf{X}_n \mathbf{f}_n \mathbf{f}_n^\dagger \mathbf{X}_n^\dagger \mathbf{V}_n^{(\ell)\dagger} \mathbf{C}_n^\dagger\right\} \\ &\quad + \mathbb{E}\{\mathbf{z}_1^{(\ell)} \mathbf{z}_1^{(\ell)\dagger}\}. \end{aligned} \quad (31)$$

Using (31) with the facts that  $\mathbf{X}_n \mathbf{X}_n^\dagger = \mathbf{I}_{M_n}$ ,  $\mathbb{E}\{\mathbf{f}_n \mathbf{f}_n^\dagger\} = \mathbf{I}_{M_n}$  and  $\mathbb{E}\{\mathbf{V}_n^{(\ell)} \mathbf{V}_n^{(\ell)\dagger}\} = M_n \mathbf{I}_N$  for linear codes and  $\mathbb{E}\{\mathbf{V}_n^{(\ell)} \mathbf{V}_n^{(\ell)\dagger}\} = M_n \mathbf{I}_{2N}$ , for sesquilinear codes,  $n = 1, \dots, N$ , yields (15).

#### B. Proof of (18)

To obtain the average received power of the desired signal, we use (11)–(13) to write

$$\begin{aligned} &\mathbb{E}\{(\mathbf{S}_2^{(\ell)} \mathbf{h}_2)^{\dagger} (\mathbf{S}_2^{(\ell)} \mathbf{h}_2)\} \\ &= \mathbb{E}\left\{\sum_{n=1}^N \sum_{q=1}^N \beta_n \beta_q \mathbf{f}_n^\dagger \mathbf{X}_n^\dagger \bar{\mathbf{g}}_n \boldsymbol{\theta}_2^{(\ell)\dagger} \mathbf{C}_n^\dagger \mathbf{C}_q \boldsymbol{\theta}_2^{(\ell)} \mathbf{g}_q^T \mathbf{X}_q \mathbf{f}_q\right\} \\ &= \mathbb{E}\left\{\sum_{n=1}^N \beta_n^2 \text{Tr}(\mathbf{X}_n^\dagger \bar{\mathbf{g}}_n \boldsymbol{\theta}_2^{(\ell)\dagger} \mathbf{C}_n^\dagger \mathbf{C}_n \boldsymbol{\theta}_2^{(\ell)} \mathbf{g}_n^T \mathbf{X}_n)\right\} \\ &= \mathbb{E}\left\{\sum_{n=1}^N \beta_n^2 \text{Tr}(\boldsymbol{\theta}_2^{(\ell)\dagger} \mathbf{C}_n^\dagger \mathbf{C}_n \boldsymbol{\theta}_2^{(\ell)}) \text{Tr}(\mathbf{X}_n^\dagger \bar{\mathbf{g}}_n \mathbf{g}_n^T \mathbf{X}_n)\right\}, \end{aligned} \quad (32)$$

where in (32) we used the fact that for  $n \neq q$ ,  $\boldsymbol{\theta}_2^{(\ell)}$ ,  $\mathbf{f}_n$ ,  $\mathbf{f}_q$ ,  $\mathbf{g}_n$  and  $\mathbf{g}_q$  are identically and independently distributed (i.i.d.) with zero mean, and we replaced the scalar  $\boldsymbol{\theta}_2^{(\ell)\dagger} \mathbf{C}_n^\dagger \mathbf{C}_n \boldsymbol{\theta}_2^{(\ell)}$  by its trace, computed expectation over  $\boldsymbol{\theta}_2^{(\ell)}$  and  $\mathbf{g}_n$ , and used (6) to obtain (18).

#### C. Proof of (19)

To obtain the average received power of the self-interference component in (10), we use an approach analogous to the one used in deriving (18) to arrive at

$$\mathbb{E}\{(\mathbf{S}_1^{(\ell)} \mathbf{h}_1)^{\dagger} (\mathbf{S}_1^{(\ell)} \mathbf{h}_1)\} = \mathbb{E}\left\{\sum_{n=1}^N N \beta_n^2 \mathbf{f}_n^\dagger \mathbf{X}_n^\dagger \bar{\mathbf{f}}_n \mathbf{f}_n^T \mathbf{X}_n \mathbf{f}_n\right\}. \quad (33)$$

To compute the RHS of (33), we denote the  $m$ -th entry of  $\mathbf{f}_n$  by  $f_{nm}$ , and the  $pq$ -th entry of  $\mathbf{X}_n$  by  $x_{pq}^{(n)}$ ,  $m, p, q = 1, \dots, M_n$ ,  $n = 1, \dots, N$ . Using this notation, we write

$$\begin{aligned} &\mathbb{E}\{\mathbf{f}_n^\dagger \mathbf{X}_n^\dagger \bar{\mathbf{f}}_n \mathbf{f}_n^T \mathbf{X}_n \mathbf{f}_n\} \\ &= \mathbb{E}\left\{\sum_{m=1}^{M_n} \sum_{q=1}^{M_n} \sum_{m_0=1}^{M_n} \sum_{q_0=1}^{M_n} f_{nm} f_{nq} \bar{f}_{nm_0} \bar{f}_{nq_0} x_{mq}^{(n)} \bar{x}_{m_0q_0}^{(n)}\right\} \\ &= \mathbb{E}\left\{\sum_{m=1}^{M_n} |f_{nm}|^4 |x_{mm}^{(n)}|^2\right\} + \mathbb{E}\left\{\sum_{m=1}^{M_n} \sum_{q=1}^{M_n} |f_{nm}|^2 |f_{nq}|^2 |x_{mq}^{(n)}|^2\right\} \end{aligned} \quad (34)$$

$$\begin{aligned}
& + \mathbb{E} \left\{ \sum_{m=1}^{M_n} \sum_{q=1}^{M_n} |f_{nm}|^2 |f_{nq}|^2 x_{mq}^{(n)} \bar{x}_{qm}^{(n)} \right\} \\
& + \mathbb{E} \left\{ \sum_{m=1}^{M_n} \sum_{m_0=1}^{M_n} f_{nm}^2 \bar{f}_{nm_0}^2 x_{mm}^{(n)} \bar{x}_{m_0 m_0}^{(n)} \right\} \quad (35)
\end{aligned}$$

$$= 2 \sum_{m=1}^{M_n} |x_{mm}^{(n)}|^2 + \sum_{m=1}^{M_n} \sum_{q=m+1}^{M_n} |x_{mq}^{(n)} + x_{qm}^{(n)}|^2, \quad (36)$$

where, to obtain (35), we used that for distinct  $m, q, m_0, q_0$ , the fading coefficients  $f_{nm}, f_{nq}, f_{nm_0}$ , and  $f_{nq_0}$ , are i.i.d. zero mean unit variance complex Gaussian random variables. This implies that the only terms that are not immediately trivial in the summations in (34) are: 1)  $m = q = m_0 = q_0$ ; 2)  $m = m_0$  and  $q = q_0$ ; 3)  $m = q_0$  and  $q = m_0$ ; and 4)  $m = q$  and  $m_0 = q_0$ , yielding the four terms of (35), respectively. To compute the first term of (35), we use

$$\begin{aligned}
\mathbb{E} \{|f_{nm}|^4\} &= \mathbb{E} \{\Re(f_{nm})^4\} + \mathbb{E} \{\Im(f_{nm})^4\} \\
&+ 2 \mathbb{E} \{\Re(f_{nm})^2\} \mathbb{E} \{\Im(f_{nm})^2\} = 2. \quad (37)
\end{aligned}$$

The computation of the second and third terms is immediate. For the last term we note that

$$\begin{aligned}
\mathbb{E} \{f_{nm}^2\} &= \mathbb{E} \{\Re(f_{nm})^2\} - \mathbb{E} \{\Im(f_{nm})^2\} \\
&+ 2 \mathbb{E} \{\Re(f_{nm})\Im(f_{nk})\} = 0. \quad (38)
\end{aligned}$$

Combining (37) and (38) with the fact that  $\mathbb{E}\{|f_{nm}|^2\} = 1$  yields (19).

#### APPENDIX B PROOF OF THEOREM 1

To obtain a lower bound on the PEP of mistaking  $\mathbf{S}_{2,a}^{(\ell)}$  for  $\mathbf{S}_{2,b}^{(\ell)}$ , we write

$$\Pr(\mathbf{S}_{2,a}^{(\ell)} \rightarrow \mathbf{S}_{2,b}^{(\ell)}) = \mathbb{E}_{\theta_1^{(\ell)}, \mathbf{h}_2} \left\{ \Pr(\mathbf{S}_{2,a}^{(\ell)} \rightarrow \mathbf{S}_{2,b}^{(\ell)} | \mathbf{h}_2, \theta_1^{(\ell)}) \right\}. \quad (39)$$

Using (16), conditioned on  $\mathbf{h}_2$  and  $\theta_1^{(\ell)}$  and the zero mean Gaussian assumption on  $\mathbf{h}_1$  and  $\mathbf{w}_1^{(\ell)}$ , the vector  $\mathbf{y}_1^{(\ell)}$  is Gaussian distributed with mean  $\sqrt{P_2} \mathbf{S}_2^{(\ell)} \mathbf{h}_2$  and conditional covariance matrix

$$\begin{aligned}
\Sigma_{\mathbf{y}_1 | \mathbf{h}_2, \theta_1^{(\ell)}} &= \mathbb{E} \{ \mathbf{y}_1^{(\ell)} \mathbf{y}_1^{(\ell)\dagger} | \mathbf{h}_2, \theta_1^{(\ell)} \} \\
&= \zeta^2 P_1 \sum_{n=1}^N \beta_n^2 \alpha_n \mathbf{C}_n \theta_1^{(\ell)} \theta_1^{(\ell)\dagger} \mathbf{C}_n^\dagger + \Sigma_{\mathbf{w}_1}, \quad (40)
\end{aligned}$$

where  $\Sigma_{\mathbf{w}_1}$  is given by (15). Using this covariance and assuming ML detection, we have

$$\begin{aligned}
& \mathbb{E}_{\theta_1^{(\ell)}, \mathbf{h}_2} \left\{ \Pr(\mathbf{S}_{2,a}^{(\ell)} \rightarrow \mathbf{S}_{2,b}^{(\ell)} | \mathbf{h}_2, \theta_1^{(\ell)}) \right\} \\
&= \mathbb{E}_{\theta_1^{(\ell)}, \mathbf{h}_2} \left\{ Q(\sqrt{\Delta_2}) \right\} \\
&\geq \mathbb{E}_{\theta_1^{(\ell)}} \left\{ Q\left(\sqrt{\mathbb{E}_{\mathbf{h}_2} \{\Delta_2\}}\right) \right\}, \\
\Delta_2 &\triangleq \frac{P_2}{2} \mathbf{h}_2^\dagger (\mathbf{S}_{2,a}^{(\ell)} - \mathbf{S}_{2,b}^{(\ell)})^\dagger \Sigma_{\mathbf{y}_1 | \mathbf{h}_2, \theta_1^{(\ell)}}^{-1} (\mathbf{S}_{2,a}^{(\ell)} - \mathbf{S}_{2,b}^{(\ell)}) \mathbf{h}_2, \quad (41)
\end{aligned}$$

where, in (41), we used that, for  $x \geq 0$ ,  $Q(\sqrt{x})$  is convex, whence  $\mathbb{E}\{Q(\sqrt{x})\} \geq Q(\sqrt{\mathbb{E}\{x\}})$  [31]. To obtain a convenient

lower bound that exposes the role of  $P$ , we will obtain a bound on  $\Sigma_{\mathbf{y}_1 | \mathbf{h}_2, \theta_1^{(\ell)}}^{-1}$ . Towards that end, we use (17) and (15) in (40) to write

$$\begin{aligned}
& \Sigma_{\mathbf{y}_1 | \mathbf{h}_2, \theta_1^{(\ell)}} \\
&= \frac{P^2}{(1 + \delta_0)P + 1} \left( \zeta^2 \sum_{n=1}^N \frac{\alpha_n \delta_n}{M_n} \mathbf{C}_n \theta_1^{(\ell)} \theta_1^{(\ell)\dagger} \mathbf{C}_n^\dagger \right. \\
&\quad \left. + \frac{1}{P} \sum_{n=1}^N \delta_n \mathbf{C}_n \mathbf{C}_n^\dagger + \frac{(1 + \delta_0)P + 1}{P^2} \mathbf{I}_N \right) \\
&\geq \frac{P^2}{(1 + \delta_0)P + 1} \left( \zeta^2 \lambda_{\min}(\theta_1^{(\ell)}) \right. \\
&\quad \left. + (1 + \delta_0 + \sum_{n=1}^N \delta_n \mu_{\min}^{(n)}) P^{-1} + P^{-2} \right) \mathbf{I}_N, \quad (42)
\end{aligned}$$

where  $\lambda_{\min}(\theta_1^{(\ell)})$  and  $\mu_{\min}^{(n)}$  are the smallest eigenvalues of  $\sum_{n=1}^N \frac{\alpha_n \delta_n}{M_n} \mathbf{C}_n \theta_1^{(\ell)} \theta_1^{(\ell)\dagger} \mathbf{C}_n^\dagger$  and  $\mathbf{C}_n \mathbf{C}_n^\dagger$ , respectively. Now, let  $\sigma_{\max}^{(a,b)}$  be the largest eigenvalue of  $\Psi(\mathbf{S}_{2,a}^{(\ell)}, \mathbf{S}_{2,b}^{(\ell)}) = (\mathbf{S}_{2,a}^{(\ell)} - \mathbf{S}_{2,b}^{(\ell)})^\dagger (\mathbf{S}_{2,a}^{(\ell)} - \mathbf{S}_{2,b}^{(\ell)})$  and let  $\hat{\sigma}_{\max} = \max_{a,b} \sigma_{\max}^{(a,b)}$ . Hence, we can write  $\Psi(\mathbf{S}_{2,a}^{(\ell)}, \mathbf{S}_{2,b}^{(\ell)}) \leq \hat{\sigma}_{\max} \mathbf{I}_N$ . Substituting from this bound and (42) into (41) yields

$$\begin{aligned}
& \mathbb{E}_{\theta_1^{(\ell)}, \mathbf{h}_2} \left\{ \Pr(\mathbf{S}_{2,a}^{(\ell)} \rightarrow \mathbf{S}_{2,b}^{(\ell)} | \mathbf{h}_2, \theta_1^{(\ell)}) \right\} \\
&\geq \mathbb{E}_{\theta_1^{(\ell)}} \left\{ Q\left(\sqrt{\mathbb{E}_{\mathbf{h}_2} \{\Delta_3\}}\right) \right\}, \\
\Delta_3 &\triangleq \frac{2^{-1} \delta_0 P ((1 + \delta_0)P + 1) \hat{\sigma}_{\max} \mathbf{h}_2^\dagger \mathbf{h}_2}{P^2 \zeta^2 \lambda_{\min}(\theta_1^{(\ell)}) + P(1 + \delta_0 + \sum_{n=1}^N \delta_n \mu_{\min}^{(n)}) + 1}. \quad (43)
\end{aligned}$$

Finally, using (43) and computing the expectation over  $\mathbf{h}_2$ , yields (23).

#### APPENDIX C PROOF OF THEOREM 3

In Lemma 1, we showed that, for the matrix  $\mathbf{X}_n$  to be simultaneously unitary and skew-symmetric, its dimension must be even. Hence, in the forthcoming proof we will assume that  $M_n = 2K$ , for some integer  $K$ . For such an  $\mathbf{X}_n$ , we will denote the eigendecomposition by

$$\mathbf{X}_n = \Phi_n \Lambda_n \Phi_n^\dagger. \quad (44)$$

In this decomposition, the diagonal matrix  $\Lambda_n \in \mathbb{C}^{2K \times 2K}$  contains the eigenvalues of  $\mathbf{X}_n$  and the columns of the unitary matrix  $\Phi_n \in \mathbb{C}^{2K \times 2K}$  contain the corresponding eigenvectors. Using (44) we will derive the structure of  $\Lambda_n$  and  $\Phi_n$  in order for  $\mathbf{X}_n$  to be unitary and skew-symmetric.

We will begin by considering  $\Lambda_n$ . We record our results in the following lemma.

*Lemma 2:* For the unitary matrix  $\mathbf{X}_n$  to be skew-symmetric, its eigenvalues must be in the form  $\pm e^{j\theta_k^{(n)}}$ , where  $\theta_k^{(n)} \in [0, 2\pi)$ ,  $k = 1, \dots, K$ ,  $n = 1, \dots, N$ .

*Proof:* To prove this lemma, we note that the  $k$ -th eigenvalue of any unitary matrix,  $\mathbf{X}_n$ , must be in the form of  $e^{j\theta_k^{(n)}}$ , where  $\theta_k^{(n)} \in [0, 2\pi)$ . Suppose that  $(e^{j\theta_k^{(n)}}, \phi_k^{(n)})$  is

an eigen pair of  $X_n$ , i.e.,  $X_n \phi_k^{(n)} = e^{j\theta_k^{(n)}} \phi_k^{(n)}$ . Now, we assert that  $(e^{j\theta_k^{(n)}}, \psi_k^{(n)})$  is an eigen pair of  $X_n^T$ , i.e.,

$$X_n^T \psi_k^{(n)} = e^{j\theta_k^{(n)}} \psi_k^{(n)}, \quad (45)$$

since the transpose operation does not affect the eigenvalues. Using the fact that  $X_n$  is skew-symmetric, i.e.,  $X_n^T = -X_n$ , we can rewrite (45) as  $X_n \psi_k^{(n)} = -e^{j\theta_k^{(n)}} \psi_k^{(n)}$ , implying that  $(-e^{j\theta_k^{(n)}}, \psi_k^{(n)})$  is also the eigen pair of  $X_n$ . Hence, the eigenvalues of any unitary skew-symmetric matrix  $X_n$  appear in the form of unit modulus antipodal pairs,  $\{\pm e^{j\theta_k^{(n)}}\}_{k=1}^K$ . ■

Now we derive the properties of the unitary matrix  $\Phi_n$  in order for  $X_n$  be unitary and skew-symmetric. We record our results in the following lemma.

*Lemma 3:* Let  $\Phi_n = [\phi_1^{(n)}, \dots, \phi_{2K}^{(n)}]$ ,  $\Phi_n \in \mathbb{C}^{2K \times 2K}$ , be the unitary matrix containing the eigenvectors of the skew-symmetric unitary matrix  $X_n$ . Then,  $\Phi_n$  has the following structure:

$$\Phi_n = \begin{bmatrix} \phi_1^{(n)} & \bar{\phi}_1^{(n)} & \dots & \phi_K^{(n)} & \bar{\phi}_K^{(n)} \end{bmatrix}. \quad (46)$$

*Proof:* Let  $(e^{j\theta_k^{(n)}}, \phi_k^{(n)})$  and  $(-e^{j\theta_k^{(n)}}, \phi_{k+1}^{(n)})$  be eigen pairs of  $X_n$ . Hence, we have

$$X_n \phi_k^{(n)} = e^{j\theta_k^{(n)}} \phi_k^{(n)}, \quad X_n \phi_{k+1}^{(n)} = -e^{j\theta_k^{(n)}} \phi_{k+1}^{(n)}, \quad \forall k. \quad (47)$$

Using  $X_n^\dagger = -\bar{X}_n$  in the first equality in (47) yields  $X_n^\dagger \bar{\phi}_k^{(n)} = -e^{-j\theta_k^{(n)}} \bar{\phi}_k^{(n)}$ . That is,  $(-e^{-j\theta_k^{(n)}}, \bar{\phi}_k^{(n)})$  is an eigen pair of  $X_n^\dagger$ . On the other hand, taking the Hermitian transpose of both sides of (44) yields  $X_n^\dagger = \Phi_n \Lambda_n^\dagger \Phi_n^\dagger$ , which implies that  $(e^{-j\theta_k^{(n)}}, \phi_k^{(n)})$  is another eigen pair of  $X_n^\dagger$ ,  $k = 1, \dots, K$ . Hence, we have shown that  $(e^{-j\theta_k^{(n)}}, \phi_k^{(n)})$  and  $(-e^{-j\theta_k^{(n)}}, \bar{\phi}_k^{(n)})$  are eigen pairs of  $X_n^\dagger$ ,  $k = 1, \dots, K$ , which subsequently implies that  $(e^{j\theta_k^{(n)}}, \phi_k^{(n)})$  and  $(-e^{j\theta_k^{(n)}}, \bar{\phi}_k^{(n)})$  are eigen pairs of  $X_n$ ,  $k = 1, \dots, K$ . Using (47), it can be readily seen that  $\phi_{k+1}^{(n)} = \bar{\phi}_k^{(n)}$ . ■

Using the result of Lemma 3, we will obtain an explicit construction for the eigenvectors matrix  $\Phi_n$ . In particular, to ensure that  $\Phi_n$  is unitary, we must have for any  $k \neq k'$ ,  $k, k' = 1, \dots, K$ ,

$$\begin{aligned} \|\phi_k^{(n)}\|^2 &= 1, \quad \phi_k^{(n)\dagger} \bar{\phi}_k^{(n)} = 0, \\ \phi_k^{(n)\dagger} \phi_{k'}^{(n)} &= 0, \quad \phi_k^{(n)\dagger} \bar{\phi}_{k'}^{(n)} = 0. \end{aligned} \quad (48)$$

To construct  $\Phi_n$ , we will express  $\phi_k^{(n)}$  in terms of its real and imaginary parts, i.e.,  $\phi_k^{(n)} = \Re(\phi_k^{(n)}) + j\Im(\phi_k^{(n)})$ . Substituting for  $\phi_k^{(n)}$  in the first equality in (48) yields

$$\|\Re(\phi_k^{(n)})\|^2 + \|\Im(\phi_k^{(n)})\|^2 = 1, \quad k = 1, \dots, K, \quad (49)$$

and substituting in the second equality in (48) yields

$$\|\Re(\phi_k^{(n)})\|^2 = \|\Im(\phi_k^{(n)})\|^2, \quad \Re(\phi_k^{(n)})^T \Im(\phi_k^{(n)}) = 0, \quad \forall k. \quad (50)$$

Combining (49) with the first equality in (50) yields  $\|\Re(\phi_k^{(n)})\|^2 = \|\Im(\phi_k^{(n)})\|^2 = \frac{1}{2}$ ,  $k = 1, \dots, K$ . The second equality in (50), says that the two vectors  $\Re(\phi_k^{(n)})$  and  $\Im(\phi_k^{(n)})$

are orthogonal. The third and fourth equalities in (48) yield that, for every  $k \neq k'$ ,  $k, k' = 1, \dots, K$ ,

$$\begin{aligned} \Re(\phi_k^{(n)})^T \Re(\phi_{k'}^{(n)}) + \Im(\phi_k^{(n)})^T \Im(\phi_{k'}^{(n)}) &= 0, \\ \Im(\phi_k^{(n)})^T \Re(\phi_{k'}^{(n)}) &= \Re(\phi_k^{(n)})^T \Im(\phi_{k'}^{(n)}), \end{aligned} \quad (51)$$

$$\begin{aligned} \Re(\phi_k^{(n)})^T \Im(\phi_{k'}^{(n)}) &= \Im(\phi_k^{(n)})^T \Re(\phi_{k'}^{(n)}), \\ \Im(\phi_k^{(n)})^T \Re(\phi_{k'}^{(n)}) + \Re(\phi_k^{(n)})^T \Im(\phi_{k'}^{(n)}) &= 0. \end{aligned} \quad (52)$$

Combining the first equality in (51) with the first equality in (52) yields that  $\Re(\phi_k^{(n)})$  and  $\Re(\phi_{k'}^{(n)})$  are orthogonal and that  $\Im(\phi_k^{(n)})$  and  $\Im(\phi_{k'}^{(n)})$  are orthogonal. Furthermore, combining the second equality in (51) with the second equality in (52) yields that  $\Re(\phi_k^{(n)})$  and  $\Im(\phi_{k'}^{(n)})$  are orthogonal and that  $\Im(\phi_k^{(n)})$  and  $\Re(\phi_{k'}^{(n)})$  are orthogonal. Hence, the vectors in the set  $\{\Re(\phi_k^{(n)}), \Im(\phi_k^{(n)}), \Re(\phi_{k'}^{(n)}), \Im(\phi_{k'}^{(n)})\}$  are mutually orthogonal for every  $k \neq k'$ ,  $k, k' = 1, \dots, K$ . This implies that to construct the  $2K \times 2K$  complex matrix  $\Phi_n$  we need a  $2K \times 2K$  real orthogonal matrix  $\mathcal{Q}_n = [\mathbf{q}_1^{(n)}, \mathbf{q}_2^{(n)}, \dots, \mathbf{q}_{2K}^{(n)}]$ , i.e., a real matrix with orthonormal columns. Using  $\mathcal{Q}_n$ , the  $k$ -th column of the desired unitary matrix  $\Phi_n$  in (46) can be constructed as  $\phi_k^{(n)} = \frac{1}{\sqrt{2}}(\mathbf{q}_{2k-1}^{(n)} + j\mathbf{q}_{2k}^{(n)})$ ,  $k = 1, \dots, K$ , which completes the proof of Theorem 3.

## APPENDIX D

### PROOF OF THEOREM 4

To obtain an upper bound on the PEP of mistaking  $U_{2,a}^{(\ell)}$  for  $U_{2,b}^{(\ell)}$ , we write

$$\Pr(U_{2,a}^{(\ell)} \rightarrow U_{2,b}^{(\ell)}) = E_{\mathbf{f}_n, \mathbf{g}_n} \left\{ \Pr(U_{2,a}^{(\ell)} \rightarrow U_{2,b}^{(\ell)} | \mathbf{f}_n, \mathbf{g}_n) \right\}. \quad (53)$$

Using (14), it can be seen that, conditioned on  $\mathbf{f}_n$  and  $\mathbf{g}_n$ , the noise vector  $\mathbf{w}_1^{(\ell)}$  is zero mean Gaussian distributed with conditional covariance matrix  $\Sigma_{\mathbf{w}_1 | \mathbf{f}_n, \mathbf{g}_n} = \sum_{n=1}^N \beta_n^2 \|\mathbf{f}_n\|^2 \mathbf{C}_n \mathbf{C}_n^\dagger + \mathbf{I}_N$ . Now, using (25), conditioned on  $\mathbf{f}_n$  and  $\mathbf{g}_n$  and the fact that  $\mathbf{y}_1^{(\ell-1)}$  was received in the  $\ell - 1$ -th block, the received vector in the  $\ell$ -th block,  $\mathbf{y}_1^{(\ell)}$ , is Gaussian distributed with mean  $U_{2,a}^{(\ell)} \mathbf{y}_1^{(\ell-1)}$  and covariance matrix  $\Sigma_{\mathbf{y}_1 | \mathbf{f}_n, \mathbf{g}_n} = 2\Sigma_{\mathbf{w}_1 | \mathbf{f}_n, \mathbf{g}_n}$ . Hence, the probability that the ML detector in (26) mistakes  $U_{2,a}^{(\ell)}$  for  $U_{2,b}^{(\ell)}$  is

$$\begin{aligned} \Pr(U_{2,a}^{(\ell)} \rightarrow U_{2,b}^{(\ell)} | \mathbf{f}_n, \mathbf{g}_n) &= Q\left(\frac{1}{\sqrt{2}} \left\| \Sigma_{\mathbf{y}_1 | \mathbf{f}_n, \mathbf{g}_n}^{-\frac{1}{2}} (U_{2,a}^{(\ell)} - U_{2,b}^{(\ell)}) \mathbf{y}_1^{(\ell-1)} \right\|\right). \end{aligned} \quad (54)$$

At high  $P$ , the noise components in (24) and (25) can be ignored and we can closely approximate  $U_{2,a}^{(\ell)} \mathbf{y}_1^{(\ell-1)}$  by  $\sqrt{P_2} \mathbf{S}_2^{(\ell)} \mathbf{h}_2$ . Using this in (54) yields

$$\begin{aligned} \Pr(\mathbf{S}_{2,a}^{(\ell)} \rightarrow \mathbf{S}_{2,b}^{(\ell)}) &= E_{\mathbf{f}_n, \mathbf{g}_n} \left\{ Q\left(\frac{1}{\sqrt{2}} \left\| \sqrt{\delta_0 P} \Sigma_{\mathbf{y}_1 | \mathbf{f}_n, \mathbf{g}_n}^{-\frac{1}{2}} (\mathbf{S}_{2,a}^{(\ell)} - \mathbf{S}_{2,b}^{(\ell)}) \mathbf{h}_2 \right\|\right) \right\} \\ &\leq E_{\mathbf{f}_n, \mathbf{g}_n} e^{-\frac{\delta_0 P}{8} \mathbf{h}_2^\dagger (\mathbf{S}_{2,a}^{(\ell)} - \mathbf{S}_{2,b}^{(\ell)})^\dagger \Sigma_{\mathbf{y}_1 | \mathbf{f}_n, \mathbf{g}_n}^{-1} (\mathbf{S}_{2,a}^{(\ell)} - \mathbf{S}_{2,b}^{(\ell)}) \mathbf{h}_2}, \end{aligned} \quad (55)$$

where in writing (55), we used the Chernoff bound for the  $Q(\cdot)$  function [2]. To obtain a more convenient upper bound that reveals the role of  $P$ ,  $M_n$ , and  $N$ , we will obtain a bound on  $\Sigma_{y_1|f_n, g_n}^{-1}$ . Using the fact that  $C_n C_n^\dagger \leq \text{Tr}(C_n C_n^\dagger) \mathbf{I}_N$  and  $\text{Tr}(C_n C_n^\dagger) = N$ , we can write

$$\Sigma_{y_1|f_n, g_n} \leq \sigma_{y_1} \mathbf{I}_N, \quad (56)$$

where  $\sigma_{y_1} = 2 \left( \frac{PN}{(1+\delta_0)P+1} \sum_{n=1}^N \frac{\delta_n}{M_n} \|f_n\|^2 + 1 \right)$ . Now, we write  $\mathbf{h}_2 = \mathbf{F} \mathbf{g}$  in (13), where

$$\mathbf{F} = \text{diag}(\beta_1 \mathbf{f}_1^T \mathbf{X}_1^T, \dots, \beta_N \mathbf{f}_N^T \mathbf{X}_N^T), \quad \mathbf{g} = [\mathbf{g}_1^T, \dots, \mathbf{g}_N^T]^T. \quad (57)$$

Substituting from (56) and (57) in (55) yields the following upper bound on the PEP:

$$\Pr(\mathbf{S}_{2,a}^{(\ell)} \rightarrow \mathbf{S}_{2,b}^{(\ell)}) \leq \mathbb{E}_{f_n, g_n} e^{-\frac{\delta_0 P}{8\sigma_{y_1}} \mathbf{g}^\dagger \mathbf{F}^\dagger \Psi(\mathbf{S}_{2,a}^{(\ell)}, \mathbf{S}_{2,b}^{(\ell)}) \mathbf{F} \mathbf{g}}, \quad (58)$$

where  $\Psi(\mathbf{S}_{2,a}^{(\ell)}, \mathbf{S}_{2,b}^{(\ell)})$  is defined in Appendix B. Computing the expectation over the entries of  $\mathbf{g}_n$ , which are i.i.d. zero-mean unit-variance complex Gaussian random variables yields [32]

$$\Pr(\mathbf{S}_{2,a}^{(\ell)} \rightarrow \mathbf{S}_{2,b}^{(\ell)}) \leq \mathbb{E}_{f_n} \left| \mathbf{I}_N + \frac{\delta_0 P}{8\sigma_{y_1}} \Psi(\mathbf{S}_{2,a}^{(\ell)}, \mathbf{S}_{2,b}^{(\ell)}) \mathbf{F} \mathbf{F}^\dagger \right|^{-1}. \quad (59)$$

At high values of  $P$ , the unity in the denominator of  $\sigma_{y_1}$  can be ignored, yielding  $\sigma_{y_1} \approx 2 \left( \frac{N}{(1+\delta_0)} \sum_{n=1}^N \frac{\delta_n}{M_n} \|f_n\|^2 + 1 \right)$ , and noting that  $\Psi(\mathbf{S}_{2,a}^{(\ell)}, \mathbf{S}_{2,b}^{(\ell)})$  is strictly positive definite, the identity matrix,  $\mathbf{I}_N$ , can be ignored in (59). Combining this with the  $\sigma_{y_1}$  yields

$$\Pr(\mathbf{S}_{2,a}^{(\ell)} \rightarrow \mathbf{S}_{2,b}^{(\ell)}) \leq \left( \frac{\delta_0 P}{16} \right)^{-N} |\Psi(\mathbf{S}_{2,a}^{(\ell)}, \mathbf{S}_{2,b}^{(\ell)})|^{-1} \times \mathbb{E}_{f_n} \{ \chi(\|f_n\|^2) \}, \quad (60)$$

where  $\chi(\|f_n\|^2) = \frac{(1+\delta_0+N \sum_{n=1}^N \frac{\delta_n}{M_n} \|f_n\|^2)^N}{\prod_{n=1}^N \frac{\delta_n}{M_n} \|f_n\|^2}$ . To compute the expectation, we consider two disjoint intervals:  $\|f_n\|^2 > M_n$  and  $\|f_n\|^2 \leq M_n$ . Using these intervals, the expectation in (60) is

$$\begin{aligned} & \mathbb{E}_{f_n} \{ \chi(\|f_n\|^2) \} \\ &= \Xi_1 \Pr(\|f_n\|^2 \leq M_n) + \Xi_2 \Pr(\|f_n\|^2 > M_n), \quad (61) \\ \Xi_1 &= \mathbb{E}_{f_n} \left\{ \chi(\|f_n\|^2) \middle| \|f_n\|^2 \leq M_n \right\}, \\ \Xi_2 &= \mathbb{E}_{f_n} \left\{ \chi(\|f_n\|^2) \middle| \|f_n\|^2 > M_n \right\}. \quad (62) \end{aligned}$$

This choice of intervals simplifies analysis, but does not necessarily yield the tightest bound. Now,  $\|f_n\|^2$  is a Chi-square random variable with  $2M_n$  degree of freedom and its CDF is

$$\Pr(\|f_n\|^2 \leq M_n) = 1 - e^{-M_n} \sum_{m=0}^{M_n-1} \frac{1}{m!} M_n^m. \quad (63)$$

To proceed, we have the following bounds on  $\Xi_1$  and  $\Xi_2$ .

*Lemma 4:* When  $\|f_n\|^2 \leq M_n$  we have the following upper bound

$$\Xi_1 \leq \frac{(1 + \delta_0 + N \sum_{n=1}^N \delta_n)^N}{\prod_{n=1}^N \delta_n}. \quad (64)$$

*Proof:* Since  $\|f_n\|^2 \leq M_n$ , we have

$$\Xi_1 \leq \mathbb{E}_{f_n} \left\{ \frac{(1 + \delta_0 + N \sum_{n=1}^N \delta_n)^N}{\prod_{n=1}^N \frac{\delta_n}{M_n} \|f_n\|^2} \right\}. \quad (65)$$

Since  $M_n$  is even (cf. Lemma 1), we have  $M_n \geq 2$ . Hence, the expectation on the RHS of (65) can be readily computed, thereby yielding the bound in the lemma. ■

*Lemma 5:* When  $\|f_n\|^2 > M_n$  we have the following upper bound

$$\Xi_2 \leq \frac{(1 + \delta_0)^N + N^N \sum_{n=1}^N \left( \frac{\delta_n}{M_n} \right)^N \frac{(N+M_n-1)!}{(M_n-1)!}}{\prod_{n=1}^N \delta_n}. \quad (66)$$

*Proof:* Since  $\|f_n\|^2 > M_n$  we have

$$\begin{aligned} \Xi_2 &\leq \mathbb{E}_{f_n} \left\{ \frac{(1 + \delta_0 + N \sum_{n=1}^N \frac{\delta_n}{M_n} \|f_n\|^2)^N}{\prod_{n=1}^N \delta_n} \right\} \\ &\leq \mathbb{E}_{f_n} \left\{ \frac{(1 + \delta_0)^N + N^N \sum_{n=1}^N \left( \frac{\delta_n}{M_n} \|f_n\|^2 \right)^N}{\prod_{n=1}^N \delta_n} \right\}, \quad (67) \end{aligned}$$

where the first inequality is obtained by using  $\|f_n\|^2 > M_n$  in the denominator of  $\Xi_2$  and the second inequality is obtained by using the Jensen's inequality. Finally, the expectation on the RHS of (67) can be readily computed, thereby yielding the bound in the lemma. ■

Substituting from (64) and (66) in (60) results in the PEP upper bound given in (27).

#### ACKNOWLEDGEMENTS

The authors would like to thank Prof. A. H. Banihashemi of Carleton University for his input.

#### REFERENCES

- [1] K. J. R. Liu, A. Sadek, W. Su, and A. Kwasinski, *Cooperative Communications and Networking*. New York, NY, USA: Cambridge Univ. Press, 2009.
- [2] Y. Jing and B. Hassibi, "Distributed space-time coding in wireless relay networks," *IEEE Trans. Wireless Commun.*, vol. 5, no. 12, pp. 3524–3536, Dec. 2006.
- [3] M. Samavat, A. Morsali, and S. Talebi, "Delay-interleaved cooperative relay networks," *IEEE Commun. Lett.*, vol. 18, no. 12, pp. 2137–2140, Dec. 2014.
- [4] V. Tarokh, H. Jafarkhani, and A. R. Calderbank, "Space-time block codes from orthogonal designs," *IEEE Trans. Inf. Theory*, vol. 45, no. 5, pp. 1456–1467, Jul. 1999.
- [5] A. Adinoyi and H. Yanikomeroglu, "Cooperative relaying in multi-antenna fixed relay networks," *IEEE Trans. Wireless Commun.*, vol. 6, no. 2, pp. 533–544, Feb. 2007.
- [6] H. Jafarkhani, *Space-Time Coding: Theory and Practice*. New York, NY, USA: Cambridge Univ. Press, 2010.
- [7] Y. Jing and H. Jafarkhani, "Distributed differential space-time coding for wireless relay networks," *IEEE Trans. Commun.*, vol. 56, no. 7, pp. 1092–1100, Jul. 2008.
- [8] B. Rankov and A. Wittneben, "Achievable rate regions for the two-way relay channel," in *Proc. IEEE Int. Symp. Inf. Theory*, Seattle, WA, USA, Jul. 2006, pp. 1668–1672.
- [9] P. Popovski and H. Yomo, "Physical network coding in two-way wireless relay channels," in *Proc. IEEE Int. Conf. Commun. (INFOCOM)*, Jun. 2007, pp. 707–712.
- [10] T. Cui, F. Gao, T. Ho, and A. Nallanathan, "Distributed space-time coding for two-way wireless relay networks," *IEEE Trans. Signal Process.*, vol. 57, no. 2, pp. 658–671, Feb. 2009.
- [11] L. Song, G. Hong, B. Jiao, and M. Debbah, "Joint relay selection and analog network coding using differential modulation in two-way relay channels," *IEEE Trans. Veh. Technol.*, vol. 59, no. 6, pp. 2932–2939, Jul. 2010.

- [12] L. Song, Y. Li, A. Huang, B. Jiao, and A. V. Vasilakos, "Differential modulation for bidirectional relaying with analog network coding," *IEEE Trans. Signal Process.*, vol. 58, no. 7, pp. 3933–3938, Jul. 2010.
- [13] T. Cui, F. Gao, and C. Tellambura, "Differential modulation for two-way wireless communications: A perspective of differential network coding at the physical layer," *IEEE Trans. Commun.*, vol. 57, no. 10, pp. 2977–2987, Oct. 2009.
- [14] S. J. Alabed, J. M. Paredes, and A. B. Gershman, "A simple distributed space-time coded strategy for two-way relay channels," *IEEE Trans. Wireless Commun.*, vol. 11, no. 4, pp. 1260–1265, Apr. 2012.
- [15] Z. Utkovski, G. Yammine, and J. Lindner, "A distributed differential space-time coding scheme for two-way wireless relay networks," in *Proc. IEEE Int. Symp. Inf. Theory*, Jun. 2009, pp. 779–783.
- [16] Q. Huo, L. Song, Y. Li, and B. Jiao, "A distributed differential space-time coding scheme with analog network coding in two-way relay networks," *IEEE Trans. Signal Process.*, vol. 60, no. 9, pp. 4998–5004, Sep. 2012.
- [17] C. Li, H. J. Yang, F. Sun, J. M. Cioffi, and L. Yang, "Multiuser overhearing for cooperative two-way multiantenna relays," *IEEE Trans. Veh. Technol.*, vol. 65, no. 5, pp. 3796–3802, May 2016.
- [18] C. Li, H. J. Yang, F. Sun, J. M. Cioffi, and L. Yang, "Adaptive overhearing in two-way multi-antenna relay channels," *IEEE Signal Process. Lett.*, vol. 23, no. 1, pp. 117–120, Jan. 2016.
- [19] C. Li, L. Yang, and W. P. Zhu, "Two-way MIMO relay precoder design with channel state information," *IEEE Trans. Commun.*, vol. 58, no. 12, pp. 3358–3363, Dec. 2010.
- [20] F. Oggier and B. Hassibi, "An algebraic coding scheme for wireless relay networks with multiple-antenna nodes," *IEEE Trans. Signal Process.*, vol. 56, no. 7, pp. 2957–2966, Jul. 2008.
- [21] F. Oggier and B. Hassibi, "Cyclic distributed space-time codes for wireless relay networks with no channel information," *IEEE Trans. Inf. Theory*, vol. 56, no. 1, pp. 250–265, Jan. 2010.
- [22] F. Oggier and B. Hassibi, "A coding scheme for wireless networks with multiple antenna nodes and no channel information," in *Proc. IEEE Int. Conf. Acoust., Speech, Signal Process.*, Apr. 2007, pp. III-413–III-416.
- [23] Y. Jing and H. Jafarkhani, "Using orthogonal and quasi-orthogonal designs in wireless relay networks," *IEEE Trans. Inf. Theory*, vol. 53, no. 11, pp. 4106–4118, Nov. 2007.
- [24] R. A. Horn and C. R. Johnson, *Matrix Analysis*. New York, NY, USA: Cambridge Univ. Press, 1985.
- [25] S. A. Zummo, P.-C. Yeh, and W. E. Stark, "A union bound on the error probability of binary codes over block-fading channels," *IEEE Trans. Veh. Technol.*, vol. 45, no. 6, pp. 2085–2093, Nov. 2005.
- [26] B. M. Hochwald and W. Sweldens, "Differential unitary space-time modulation," *IEEE Trans. Commun.*, vol. 48, no. 12, pp. 2041–2052, Dec. 2000.
- [27] F. Behnamfar, F. Alajaji, and T. Linder, "Tight error bounds for space-time orthogonal block codes under slow Rayleigh flat fading," *IEEE Trans. Commun.*, vol. 53, no. 6, pp. 952–956, Jun. 2005.
- [28] S. M. Alamouti, "A simple transmit diversity technique for wireless communications," *IEEE J. Sel. Areas Commun.*, vol. 16, no. 8, pp. 1451–1458, Oct. 1998.
- [29] Y. Jing and B. Hassibi, "Design of fully diverse multiple-antenna codes based on  $Sp(2)$ ," *IEEE Trans. Inf. Theory*, vol. 50, no. 11, pp. 2639–2656, Nov. 2004.
- [30] W. C. Jakes and D. C. Cox, *Microwave Mobile Communications*. Piscataway, NY, USA: Wiley, 1994.
- [31] S. Boyd and L. Vandenberghe, *Convex Optimization*. Cambridge, U.K.: Cambridge Univ. Press, 2004.
- [32] A. Dogandzic, "Chernoff bounds on pairwise error probabilities of space-time codes," *IEEE Trans. Inf. Theory*, vol. 49, no. 5, pp. 1327–1336, May 2003.



**Salime Bameri** (S'11) received the B.Sc. degree in electrical engineering and the M.Sc. degree in communications engineering from Shahid Bahonar University of Kerman, Kerman, Iran, in 2009 and 2013, respectively. She is currently pursuing the Ph.D. degree in communications engineering from Shahid Bahonar University of Kerman in collaboration with Carleton University, Ottawa, ON, Canada. Her research interests include MIMO system, space-time-frequency coding, cooperative communication systems, distributed space-time-frequency coding, and distributed differential coding.



**Siamak Talebi** received the B.S. and M.S. degrees in communication engineering from the Isfahan University of Technology, in 1989 and 1992, respectively, and the Ph.D. degree from King's College London in 2001. He is currently with the Department of Electrical Engineering, Shahid Bahonar University of Kerman, Iran. He is also with the Advanced Communications Research Institute, Sharif University of Technology, Tehran, Iran. His research interests are wireless communications, MIMO-OFDM, source allocation for cooperative cognitive networks, and also video coding.



**Ramy H. Gohary** (SM'13) received the B.Eng. degree (Hons.) from Assiut University, Egypt, in 1996, the M.Sc. degree from Cairo University, Egypt, in 2000, and the Ph.D. degree from McMaster University, Canada, in 2006, all in electronics and communications engineering. He is currently an Assistant Professor with the Department of Systems and Computer Engineering, and a member of the College of Reviewers and the Panel Review Board of the Ontario Centre of Excellence.

He has co-authored over 90 IEEE journal and conference papers, and co-supervised over ten Ph.D. and master's students. He is a co-inventor of five U.S. patents. His research interests include applications of embedded systems in machine-to-machine communications, Internet-of-Things, cross-layer design of wireless networks, analysis and design of MIMO wireless communication systems, applications of optimization and geometry in signal processing and communications, information theoretic aspects of multiuser communication systems, and applications of iterative detection and decoding techniques in multiple antenna and multiuser systems.

Dr. Gohary has been named the Best Professor by the Carleton Student Engineering Society for 2015. He is a registered Limited Engineering Licensee in the Province of Ontario, Canada.



**Halim Yanikomeroglu** (F'17) was born in Giresun, Turkey, in 1968. He received the B.Sc. degree in electrical and electronics engineering from Middle East Technical University, Ankara, Turkey, in 1990, and the M.A.Sc. degree in electrical engineering (now ECE) and the Ph.D. degree in electrical and computer engineering from the University of Toronto, Canada, in 1992 and 1998, respectively.

From 1993 to 1994, he was with the Research and Development Group, Marconi Kominikasyon A.S., Ankara, Turkey. Since 1998, he has been with the Department of Systems and Computer Engineering, Carleton University, Ottawa, Canada, where he is currently a Full Professor. His research interests cover many aspects of wireless technologies with a special emphasis on cellular networks. In recent years, his research has been supported by Huawei, Telus, Allen Vanguard, Blackberry, Samsung, Communications Research Centre of Canada, and DragonWave. This collaborative research resulted in about 30 patents (granted and applied). He is a Distinguished Lecturer of the IEEE Communications Society and a Distinguished Speaker for the IEEE Vehicular Technology Society in 5G wireless technologies. He has been involved, in various capacities, in the organization of the IEEE Wireless Communications and Networking Conference (WCNC) since its inception in 1998, including serving as a steering committee member, an executive committee member and the Technical Program Chair or the Co-Chair of the WCNC 2004, Atlanta, GA, USA, the WCNC 2008, Las Vegas, NV, USA, and the WCNC 2014, Istanbul. He was the General Co-Chair of the IEEE Vehicular Technology Conference (VTC2010-Fall) held in Ottawa and the General Chair IEEE VTC2017-Fall held in Toronto. He has served on the editorial boards of the IEEE TRANSACTIONS ON COMMUNICATIONS, the IEEE TRANSACTIONS ON WIRELESS COMMUNICATIONS, and the IEEE Communications Surveys and Tutorials. He was the Chair of the IEEE Wireless Technical Committee.

Dr. Yanikomeroglu was a recipient of the IEEE Ottawa Section Outstanding Educator Award in 2014, the Carleton University Faculty Graduate Mentoring Award in 2010, the Carleton University Graduate Students Association Excellence Award in Graduate Teaching in 2010, and the Carleton University Research Achievement Award in 2009. He was a Visiting Professor with the TOBB University of Economics and Technology, Ankara, Turkey, from 2011 to 2012. He is a registered professional engineer in Ontario, Canada.